Desalination and Water Treatment
www.deswater.com
doi: 10.5004/dwt.2022.28841

273 (2022) 13–33
October

Influence of dissimilarity of water depth on performance of N alike photovoltaic thermal flat plate collectors included with double slope solar still: a comparative study

Devesh Kumar[a], R.K. Sharma[b], Sanjeev Kumar Sharma[c], Vijay Kumar Dwivedi[a], Sumit Tiwari[d], Desh Bandhu Singh[e,*]

[a]*Madan Mohan Malviya University of Technology, Gorakhpur – 273010, UP, India, email: dkme@mmmut.ac.in*
[b]*University of Petroleum and Energy Studies (UPES), Bidholi, Premnagar, Dehradun – 248007, Uttarakhand, India, email: ram.sharma@upes.ac.in*
[c]*Department of Mechanical Engineering, Amity University Uttar Pradesh, Noida, India, email: sksharma6@amity.edu*
[d]*Department of Mechanical Engineering, Shiv Nadar Institution of Eminence, Greater Noida, UP, India, email: sumit.tiwari@snu.edu.in*
[e]*Department of Mechanical Engineering, Graphic Era Deemed to be University, Bell Road, Clement Town, Dehradun – 248002, Uttarakhand, India, email: dbsiit76@gmail.com/deshbandhusingh.me@geu.ac.in*

Received 22 April 2021; Accepted 10 August 2022

ABSTRACT

This research work communicates the influence of dissimilarity of water depth on various efficiencies and productivity of N alike photovoltaic thermal flat plate collectors included with double slope solar still (NPVTFPC-DS). The analysis for NPVTFPC-DS has been done taking normal days of June and January for climatical condition of New Delhi into consideration. The hourly thermal, exergy, electrical and overall exergy efficiencies and productivity have been calculated for distinct values of water depth followed by the calculation of their mean values under optimized values of number of collectors (N = 11) and mass flow rate ($\dot{m}_f$ = 0.03 kg/s). The values of average daily efficiencies and productivity first increase and then they become almost constant beyond water depth of 0.70 m. Values of various thermal efficacies and productivity obtained for NPVTFPC-DS has been compared with corresponding values for the similar set up of single slope type and it has been concluded that the values of exergy efficiency, thermal efficacy and productivity for NPVTFPC-DS are higher by 17.65%, 2.89% and 2.42% respectively than similar set up of single slope type at water depth of 0.14 m under optimum values of N and $\dot{m}_f$.

Keywords: Exergy; Efficiency; Productivity; PVTFPC; Double slope solar still

1. Introduction

The analysis of solar still is the demand of contemporary time as the world is facing the issue of water deficiency. This type of system has the potential of purifying even seawater and the purified water can be used for different applications like industry, agriculture, hospitals, educational systems and drinking water after adding the required mineral. The renewable source of energy is a gift to nature and its wise use has the potential to solve

* Corresponding author.

the crisis of energy as well as fresh water on global level. The researchers around the globe have contributed a lot towards the development of water purification system. The relevant contribution in the present context can be summarized in the paragraphs that follow.

The contribution made by Rai and Tiwari [1] is considered as the first use of active solar still. They reported the substantial enhancement in the production of fresh water (24%) over the conventional solar still due to the addition of heat by collector to water in basin. Further, Tiwari and Dhiman [2] reported the experimental investigation of solar still containing heat exchanger and coupled to collectors. The thermal modeling of the active type of solar still was performed, and the theoretical results were experimentally validated. There was an enhancement of 12% in the production of fresh water as the length of heat exchanger was increased by 100%, that is, from 6 to 12 m due to increase in the amount of heat transfer to water in the basin with the increase in length as the fluid passing through heat exchanger tubes would be in contact for longer period. On the basis of theoretical results, an empirical relation for heat transfer coefficient of solar still was obtained by Lawrence and Tiwari [3] and reported. A study on solar still of basin type was made by Hamadou and Abdellatif [4] in which heat transfer medium (fluid) was circulated at the lower portion of the system and a non-linear relationship between freshwater production and heat transfer was obtained.

The basin type solar still coupled to two numbers of flat plate collectors was experimentally investigated by Tiris et al. [5] and reported an enhancement of 100% in the production of fresh water over the conventional basin type solar still due to heat addition by collector to the water kept in basin. The production of fresh water decreases with the increase in water depth during sunshine hours due to sensible heat storage by water mass; however, the production of fresh water was found to enhance with the enhancement in solar intensity as reported by Badran and Al-Tahainesh [6]. In another investigation, Tripathi and Tiwari [7] concluded that the convective mode of heat transfer was the function of water depth in basin and the production of fresh water was higher during off sunshine hours than the production of fresh water during sunshine hours due to the storage of sensible heat content during sunshine hours. Badran et al. [8] reported an enhancement of 52% over the conventional solar still in a similar investigation of basin type solar still. Khalifa and Hamood [9] studied single slope solar still in passive mode theoretically and consequently validated results experimentally. They concluded that the freshwater yielding was decreased with the increase in water depth during daytime due to increase in sensible heat storage by water mass in the basin. The recommendation of higher water depth in the case of active solar still was made by Taghvaei et al. [10]. The optimization using simulation method for basin type solar still coupled to PVT collectors was made by Saeedi et al. [11] and reported the optimum values of mass flow rate ($\dot{m}_f$) and number of solar collectors (N) as 0.044 kg/s and seven in that order.

Sahota and Tiwari [12] reported review on the performance analysis of solar still by incorporating PVT in active mode and result so obtained helped immensely in locating the research gap. Veeramanikandan et al. [13] did thermal modeling followed by experimental validation of sandwich-glazed photovoltaic thermal (SGPV/T) system and reported that there was a fair agreement between theoretical and experimental values of performance parameters. Kumar and Tiwari [14] performed experimentation on solar still and it was concluded that the solar still in active mode produced 3.5 times more fresh water as compared to the conventional solar still. After Kumar and Tiwari [14], Tiwari et al. [15] and Singh et al. [16] did experimentation of single slope solar still (SS) by incorporating PVT integrated flat pate collectors (FPCs) and it was reported that thermal efficacy obtained was less than that of the system reported by Kumar and Tiwari [14]; however, exergy and overall efficacies were better. Feilizadeh et al. [17] investigated single slope solar still and reported that the nocturnal yield was increased with the increase in water mass in the basin due to sensible heat storage in daytime.

Kabeel et al. [18] investigated solar still of pyramid type having titanium oxide coated absorber and concluded that freshwater yielding was 6.06% higher with coated absorber over uncoated absorber due to improvement in thermophysical property. It was also concluded that daily freshwater yielding was increased with the increase in water depth due to sensible heat storage of water mass. An investigated of solar still of tubular type for daytime was done and it was concluded that the freshwater yielding was higher for lower depth during daytime due to solar energy absorption of water mass in the form of sensible heat [19]. Issa and Chang [20] did experimentation on SS by incorporating evacuated tubes arranged in mixed mode. They concluded that the freshwater production of the reported system was 2.36 times more than passive SS because of the addition of extra heat to the basin in the case of active mode of operation. Singh [21] did experimentation on basin type solar still by incorporating (a) partially covered PVT -FPCs, (b) partially covered PVT compound parabolic concentrators (CPC) and it was concluded that life cycle conversion efficiency for solar still by incorporating PVTFPCs was higher by 37.5% and 56.25% over the SS by incorporating PVTCPC and conventional type of solar still because of higher exergy obtained for solar still integrated with PVTFPCs. It was further reported that the life cycle conversion efficiency for solar still by incorporating evacuated tubular collector (ETC) was higher than solar still in passive mode due to higher exergy gain by system consisting of ETC as heat was added to the basin in the case of active mode [22]. Fathy et al. [23] reported that the efficacy of double slope solar still (DS) by incorporating tracked parabolic trough collector was 29.6% higher than solar still containing non tracked type collector due to capture of higher solar energy in the case of tracked solar collectors.

The development of characteristic equations for SS were reported by Singh and Tiwari [24] and Kumar et al. [25] by incorporating ETCs and CPCETCs separately and it was concluded that the performance of SS by incorporating CPCETCs was better than SS by incorporating ETCs because of the enhancement in heat collection region. Prasad et al. [26] carried out the sensitivity analysis of DS in active mode of operation and it was concluded that the generation of electricity increased by 0.95% if water depth

was altered from 0.07 m to 0.14 m for the considered values of $\dot{m}_f$ and N because of reduced cell temperature at increased water depth. Singh et al. [27] studied the influence of water mass on the performance of SS by incorporating PVTFPCs and it was concluded that the augmentation in efficacy based on one day and productivity was considerable till water depth of 1.4 m. Singh et al. [28] studied the effect of variation of various parameters on SS by incorporating PVTCPCs and it was concluded that there was an increment of 81.63% corresponding to the increase in packing factor by 50%, that is, 0.4 to 0.6. Manokar et al. [29] and Modi et al. [30] investigated respectively for solar still of pyramid type and spherical type and reported that the yield is higher at lower water depth during daytime due to sensible heat of water in the basin.

Modi et al. [31] investigated double basin type SS with/without nanofluid and concluded that the use of aluminum oxide (0.01%) based nanofluid increases the production of fresh water by 17.6% compared to similar system without nanofluid. Kabeel et al. [32] have reviewed the different modifications in the design of inclined solar still with an aim to increase the productivity. Pal and Dev [33] validated theoretical results for modified SS and found a fair agreement between theoretical and experimental values. They reported the overall thermal efficiency as 26.89%. Groenewoudt et al. [34] have studied empirical analysis of solar stills in Uganada and concluded that a low quality solar still may help in the energy transition. Ye et al. [35] have invested SS for its use in agriculture experimentally and reported that the solar energy utilization was 22%. Sivaram et al. [36] studied the solar still coupled to solar chimney experimentally and concluded that the overall efficacy of chimney got improved by 37.1% in summer and 14.5% in winter.

Mohammadi et al. [37] have investigated DS by incorporating new design of heat exchanger experimentally and concluded that the production of fresh water got improved by 34.1% as compared to freshwater production from DS by incorporating parallel channel heat exchanger due to better interaction of hot fluid with water in the basin. Fallahzadeh et al. [38] have studied the active solar still by incorporating closed-loop pulsating heat pipe and concluded that the yield was 2.33 kg/m^2 area on per day basis. Essa et al. [39] have applied artificial neural network technology to active solar still for prediction of freshwater production from solar still operating in active mode. Maliani et al. [40] have reported the investigation of solar still consisting of parabolic trough collector in which provision of solar tracking system about two axes was done and reported the daily production of fresh water as 3.76 kg. The thermal modeling of DS in active mode was done by Gupta et al. [41] and they concluded that the instantaneous efficiency of solar still in active mode was higher than conventional solar still due to the addition of heat by collectors to the basin. Recently, Bharti et al. [42] have reported the sensitivity analysis of DS by incorporating N alike PVTFPCs and concluded that this type of analysis is helpful to designer as the designer will have information before installing the system as which parameter is more significant and according decide values of various parameters. Sharma et al. [43] carried out experimental validation of single slope active solar still and it was reported that the correlation coefficient for yield was 0.9951. Purnachandrakumar et al. [44] reviewed solar still using CFD and concluded that CFD was valuable tool for the analysis of solar still. Kumar et el. [45] and Raturi et al. [46] have reported the effect of variation of $\dot{m}_f$ and N on active solar still and concluded that the thermal performance of solar still without PVT was better because of the reduced area of PVT.

The extant research suggests that the dissimilarity of different types of efficiencies and productivity with water depth for N alike series connected partially covered photovoltaic thermal flat plate collectors coupled to solar still of double slope (NPVTFPC-DS) has not been reported by any researcher around the globe. Hence, this research article deals with the influence of dissimilarity of water depth on efficiencies and productivity for the proposed system. The main objective can be stated as follows:

- To compute thermal efficacy, exergy efficacy, electrical exergy efficacy, overall exergy efficacy and productivity on per hour basis followed by the computation of their daily values at optimum number of PVTFPCs and $\dot{m}_f$ for various values of water depth for NPVTFPC-DS.
- To compute average thermal efficacy on per day basis, average exergy efficacy on per day basis, average electrical exergy efficacy on per day basis, average overall exergy efficacy on per day basis and average productivity on per day basis at optimum number of PVTFPCs and $\dot{m}_f$ for various values of water depth for NPVTFPC-DS.

2. Description of NPVTFPC-DS

The arrangement of different components of the system is depicted as Fig. 1 and the specification of system is presented in Table 1. Here, PVTFPCs have been arranged in series with an objective of realizing elevated temperature of fluid at the exit of last NPVTFPC. The solar still of double slope in active mode has been oriented east-west to get maximum annual energy for New Delhi location. When solar energy impinges on the system, fluid passing through collector gains heat from the solar energy and transfers the same to water in the basin of DS. The solar intensity falling on the surface of DS gets reflected first and then absorbed by the condensing surface and the remaining part (approximately 95%) is transmitted to water in the basin. Again, some part of intensity is reflected by water, some part is absorbed by water and the remaining part is transmitted to the blackened surface at the bottom (basin liner); where, almost all solar radiation gets absorbed by the surface resulting in the increase in temperature of the blackened surface. The temperature of this surface becomes even higher than water and heat in turn is transferred to water from basin liner. In this way, water receives heat from NPVTFPCs, directly from sunlight and indirectly from basin liner resulting in the increase in temperature of water which generates a difference of temperature between water surface and condensing surface. This difference of temperatures compels water to evaporate. The vapor gets condensed at the inner side of glass through film-wise condensation and trickles down to the channel fixed at lower sides and then siphoning off the freshwater to the measuring jar is done.

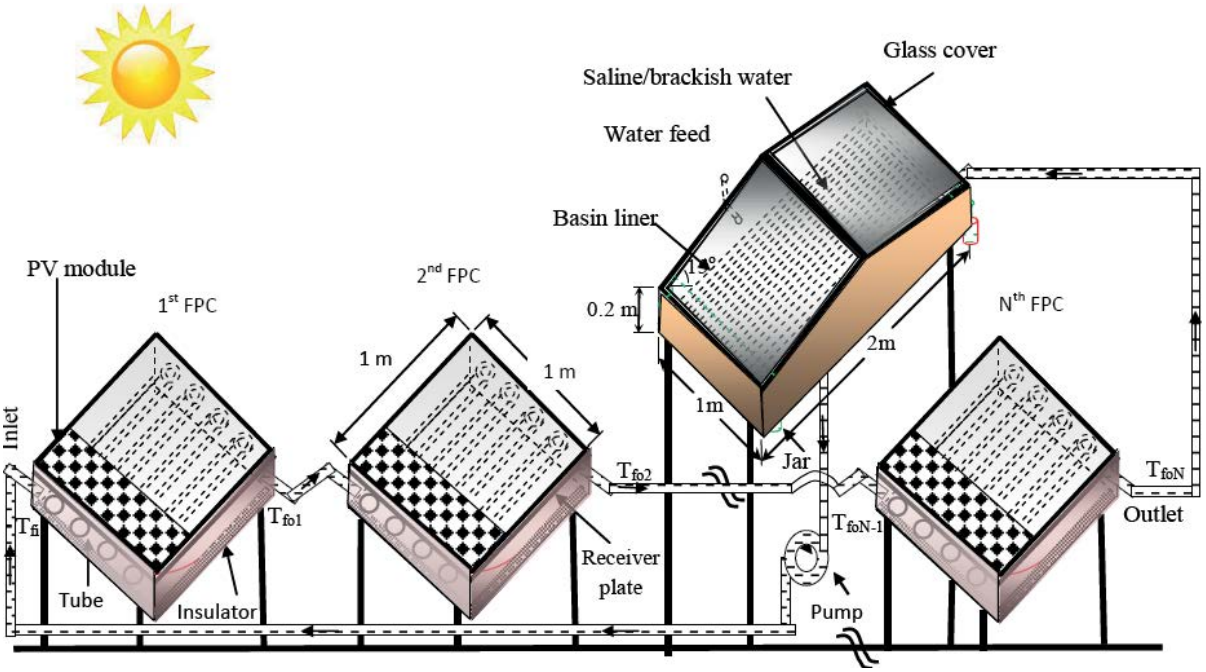

Fig. 1. Schematic representation of NPVTFPC-DS.

Table 1
Specifications of solar energy operated water purifier of double slope type coupled to N alike PVTFPCs

Solar energy operated water purifier of double slope type			
Component	Specification	Component	Specification
Length	2 m	Cover material	Glass
Width	1 m	Orientation	East-west
Inclination of glass cover	15°	Thickness of glass cover	0.004 m
Height of smaller side	0.2 m	K_g	0.816 W/m-K
Material of body	GRP	Thickness of insulation	0.1 m
Material of stand	GI	Thermal conductivity of insulation	0.166 W/m-K
PVTFPC			
Component	Specification	Component	Specification
Type and no. of collectors	Tube in plate type, N	Area of module	0.25 m × 1.0 m
Area of solar collector	1.0 m × 1.0 m	Area of one solar cell	0.007 m^2
Collector plate thickness	0.002 m	Maximum power rating	32 W
Thickness of copper tubes	0.00056 m	F'	0.968
Length of each copper tubes	1.0 m	τ_g	0.95
Thickness of insulation	0.1 m	α_c	0.9
Angle of FPC with horizontal	30°	β_c	0.89
Thickness of toughen glass on FPC	0.004 m	α_p	0.8
Effective area of collector under glass	0.75 m^2	K_i (W^{m-1} K^{-1})	0.166
DC motor rating	12 V, 24 W	FF	0.8
		Pipe diameter	0.0125 m

3. Mathematical relations

For obtaining typical equations for NPVTFPC-DS, equations based on making balance on input energy to output energy are written taking all components one by one. Further, equations so obtained are simplified and unknown parameters are expressed in terms of known parameters like solar intensity, surrounding temperature, heat transfer coefficients and some constants. Assumptions

for developing typical equations for NPVTFPC-DS are like that of assumptions mentioned in Gupta et al. [47].

The expression for temperature at the outlet of Nth PVTFPC can be given by [48]:

$$T_{\text{fo1}} = \frac{\left(AF_R\left(\alpha\tau\right)\right)_1}{\dot{m}_f C_f} I\left(t\right) + \frac{\left(AF_R U_L\right)_1}{\dot{m}_f C_f} T_a + K_k T_{\text{fi}} \tag{1}$$

As N number of PVTFPCs have been arranged in series, the output of first PVTFPC will be input to second PVTFPC, output of second PVTFPC will be input to the third PVTFPC and so on. Following Shyam et al. [48], the temperature at the output of Nth PVTFPC (T_{foN}) can be expressed as:

$$T_{\text{foN}} = \frac{\left\{AF_R\left(\alpha\tau\right)\right\}_1}{\dot{m}_f C_f}\left(\frac{1-K_K^N}{1-K_K}\right) I\left(t\right) + \frac{\left\{AF_R U_L\right\}_1}{\dot{m}_f C_f}\left(\frac{1-K_K^N}{1-K_K}\right) T_a + T_{\text{fi}} K_K^N \tag{2}$$

After obtaining the value of T_{foN}, one can obtain the useful heat gain $\left(\dot{Q}_{\text{uN}}\right)$ for NPVTFPCs as:

$$\dot{Q}_{\text{uN}} = \dot{m}_f C_f \left(T_{\text{foN}} - T_{\text{fi}}\right) \tag{3}$$

Using Eqs. (2) and (3), one can obtain the expression of $\dot{Q}_{\text{uN}}$ as:

$$\dot{Q}_{\text{uN}} = N\left(A_c + A_m\right)\left[\left(\alpha\tau\right)_{\text{eff},N} I\left(t\right) - U_{\text{LN}}\left(T_{\text{fi}} - T_a\right)\right] \tag{4}$$

where T_{fi} stands for temperature at the bay of first PVTFPC. Here, the variable $T_{\text{fi}} = T_w$ as water inlet to 1st PVTFPC directly comes from basin through pump due to the existence of closed loop. Also, basin received hot water from the exit of Nth PVTFPC. Hence, $T_{\text{wo}} = T_{\text{foN}}$. Different unidentified terms present in Eqs. (1)–(4) are given in Appendix-A.

The mathematical relations for numerous elements of DS can be composed; and equations for different components so obtained can be simplified using Eq. (4) for getting water temperature (T_w), temperature at inside/outside surface of glass towards east ($T_{\text{giE}}/T_{\text{goE}}$) and temperature at inside/outside surface of glass towards west ($T_{\text{giW}}/T_{\text{goW}}$) as follows [49,50]:

$$T_w = \frac{\overline{f_2}\left(t\right)}{a_2}\left(1 - e^{-a_2 t}\right) + T_{w0} e^{-a_2 t} \tag{5}$$

$$T_{\text{giE}} = \frac{A_1 + A_2 T_w}{P} \tag{6}$$

$$T_{\text{giW}} = \frac{B_1 + B_2 T_w}{P} \tag{7}$$

$$T_{\text{goE}} = \frac{\frac{K_g}{L_g} T_{\text{giE}} + h_{1\text{gE}} T_a}{\frac{K_g}{L_g} + h_{1\text{gE}}} \tag{8}$$

$$T_{\text{goW}} = \frac{\frac{K_g}{L_g} T_{\text{giW}} + h_{1\text{gW}} T_a}{\frac{K_g}{L_g} + h_{1\text{gW}}} \tag{9}$$

Various unknown terms used in Eqs. (5)–(9) have been presented in Appendix-A.

After evaluating the value of T_w and glass temperatures (T_{giE} and T_{giW}), the hourly yield ($\dot{m}_{\text{ew}}$) can be evaluated as:

$$\dot{m}_{\text{ew}} = \frac{h_{\text{ewgE}} \frac{A_b}{2}\left(T_w - T_{\text{giE}}\right) + h_{\text{ewgW}} \frac{A_b}{2}\left(T_w - T_{\text{giW}}\right)}{L} \times 3{,}600 \tag{10}$$

where L stands for latent heat. The value of freshwater production on per day basis can be evaluated by accumulating freshwater production on per hour basis for 24 h. The evaporative heat transfer coefficient (h_{ewg}) can be calculated as [51,52]:

$$h_{\text{ewg}} = 16.273 \times 10^{-3} h_{\text{cwg}} \left[\frac{P_w - P_{\text{gi}}}{T_w - T_{\text{gi}}}\right] \tag{11}$$

$$\text{Here, } h_{\text{cwg}} = 0.884\left[\left(T_w - T_{\text{gi}}\right) + \frac{\left(P_w - P_{\text{gi}}\right)\left(T_w + 273\right)}{\left(268.9 \times 10^3 - P_w\right)}\right] \tag{12}$$

$$P_w = \exp\left[25.317 - \frac{5{,}144}{\left(T_w + 273\right)}\right] \tag{13}$$

$$P_{\text{gi}} = \exp\left[25.317 - \frac{5{,}144}{\left(T_{gi} + 273\right)}\right] \tag{14}$$

Hourly thermal exergy ($\dot{\text{E}}\text{x}_{\text{thermal}}(t)$) for NPVTFPC-DS can be estimated as [53–55]:

$$\dot{\text{E}}\text{x}_{\text{thermal}}\left(t\right) = \frac{A_b}{2}\left[\begin{array}{l} h_{\text{ewgE}} \times \left\{\left(T_w - T_{\text{giE}}\right) - \left(T_a + 273\right) \times \ln\frac{\left(T_w + 273\right)}{\left(T_{\text{giE}} + 273\right)}\right\} \\ + h_{\text{ewgW}} \times \left\{\left(T_w - T_{\text{giW}}\right) - \left(T_a + 273\right) \times \ln\frac{\left(T_w + 273\right)}{\left(T_{\text{giW}} + 273\right)}\right\} \end{array}\right] \tag{15}$$

$$\dot{\text{E}}\text{x}_c\left(t\right) = \dot{m}_f \times C_f \times \left[\left(T_{\text{foN}} - T_{\text{fi}}\right) - \left(T_a + 273\right) \times \ln\frac{\left(T_{\text{foN}} + 273\right)}{\left(T_{\text{fi}} + 273\right)}\right] \tag{16}$$

The daily exergy can be estimated by totaling hourly exergy for 24 h utilizing Eq. (15).

In the reported system, the fluid coming from the first PVTFPC is made input to the second PVTFPC; the fluid coming from the second PVTFPC is made input to the third PVTFPC and so on. The heated water obtained from the last (Nth) PVTFPC is allowed to go to the basin where heated water obtained from last PVTFPC gets mixed with water kept

in the basin and there is further rise in the temperature of water kept in the basin. Then, heated water of basin flows to the bay of first PVTFPC using pump. In this way, collectors make a closed loop with solar still of double slope type using DC motor pump. Here, different efficacies and productivity are evaluated for optimum values of $\dot{m}_f$ and N for a particular value of water depth in basin.

The value of electrical exergy on per hour basis NPVTFPC-DS can be computed as:

$$\dot{\mathrm{E}}\mathrm{x}_e = A_m I(t)\sum_{1}^{N}\left(\alpha\tau_g\eta_{\mathrm{cN}}\right) \tag{17}$$

where, η_{cN} is the electrical efficiency of solar cell, A_m represents the area of module and $I(t)$ is the solar intensity falling on the surface of collector.

Eq. (2) was validated by Shyam et al. [56] and Eqs. (2)–(9) were validated by Dwivedi and Tiwari [57] considering $N = 0$. These can be discussed as follows:

Shyam et al. [56] have validated temperature at the outlet of Nth collector of NPVTFCs taking value of N as 3. They collected data for temperature of fluid on April 2, 2015. They found a fair agreement between theoretical and experimental values. The percentage error was reported as 9.75%. Equations reported by Shyam et al. [56] have been used in this work keeping in mind that the proposed system forms a closed loop.

For $N = 0$, NPVTFPCDS reduces to system reported by Dwivedi and Tiwari [57]. They calculated heat transfer coefficient using Dunkle's relation similar to the computation presented in the present analysis. The validation of heat transfer coefficient as well as yield was done by them, and they found a fair agreement between theoretical and experimental values.

4. Analysis

The performance analysis of NPVTFPC-DS by inclusion of dissimilarity of water depth can be carried out as follows:

4.1. Thermal efficacy

The thermal efficacy can be computed taking first law of thermodynamics as the basis. The values of hourly and daily thermal efficiencies of NPVTFPC-DS can be expressed as follows [58–60]:

$$\eta_{\mathrm{hourly,thermal}} = \frac{\left(\dot{m}_{\mathrm{ewE}} + \dot{m}_{\mathrm{ewW}}\right)\times L}{\left[\dot{Q}_{\mathrm{uN}}(t) + \frac{A_b}{2}\left(I_{\mathrm{sE}}(t) + I_{\mathrm{sW}}(t)\right)\right]\times 3{,}600}\times 100 \tag{18}$$

$$\eta_{\mathrm{daily,thermal}} = \frac{\sum_{t=1}^{24}\left(\dot{m}_{\mathrm{ewE}} + \dot{m}_{\mathrm{ewW}}\right)\times L}{\sum_{t=1}^{24}\left[\dot{Q}_{\mathrm{uN}}(t) + \frac{A_b}{2}\left(I_{\mathrm{sE}}(t) + I_{\mathrm{sW}}(t)\right)\right]\times 3{,}600}\times 100 \tag{19}$$

where $\dot{Q}_{\mathrm{uN}}(t)$ is heat gain from NPVTFPCs on hourly basis and it can be estimated utilizing Eq. (2). The value of production of fresh water on per hour basis from NPVTFPC-DS has been evaluated considering Eqs. (8)–(10). Here, one can note that values of solar flux, useful heat gain and pump work used in Eqs. (18) and (19) are zero for nighttime (off-sunshine hours). However, the production of fresh water from NPVTFPC-DS will continue to get collected during nighttime also due to sensible heat stored by water mass during daytime. The value of latent heat is considered as 2,400 kJ/kg.

4.2. Exergy efficacy

The value of exergy efficiency can be computed by utilizing 1st as well as 2nd law of thermodynamics. The value of exergy efficiency on per hour as well as per day basis for NPVTFPC-DS has been computed as follows [58–60]:

$$\eta_{\mathrm{hourly,exergy}} = \frac{\dot{\mathrm{E}}\mathrm{x}_{\mathrm{thermal}}(t)}{\dot{\mathrm{E}}\mathrm{x}_{\mathrm{c}}(t) + \left[0.933\times\frac{A_b}{2}\times\left(I_{\mathrm{SE}}(t) + I_{\mathrm{SW}}(t)\right)\right]}\times 100 \tag{20}$$

$$\eta_{\mathrm{daily,exergy}} = \frac{\sum_{t=1}^{24}\left[\dot{\mathrm{E}}\mathrm{x}_{\mathrm{thermal}}(t)\right]}{\sum_{t=1}^{24}\left[\dot{\mathrm{E}}\mathrm{x}_{c}(t) + \left[0.933\times\frac{A_b}{2}\times\left(I_{\mathrm{SE}}(t) + I_{\mathrm{SW}}(t)\right)\right]\right]}\times 100 \tag{21}$$

where $\dot{\mathrm{E}}\mathrm{x}_c(t)$ is the hourly exergy gain from a number (N) of PVTFPCs connected in series which can be computed using Eq. (16). Here, the value of solar flux has been multiplied by 0.933 to get the value of corresponding exergy and the factor 0.933 used in Eqs. (19) and (20) can be computed using the expression reported by Petela [61].

4.3. Electrical exergy efficacy

The electrical exergy efficiency of NPVTFPC-DS can be expressed as:

$$\eta_{\mathrm{hourly,electrical\ exergy}} = \frac{\dot{\mathrm{E}}\mathrm{x}_e(t) - \dot{P}_u(t)}{0.933\times A_m\times N\times I(t)}\times 100 \tag{22}$$

$$\eta_{\mathrm{daily,electrical\ exergy}} = \frac{\sum_{t=1}^{24}\left(\dot{\mathrm{E}}\mathrm{x}_e - \dot{P}_u\right)}{0.933\times\sum_{t=1}^{t=24}\left[A_m\times N\times I(t)\right]}\times 100 \tag{23}$$

where $\dot{P}_u(t)$, N, $I(t)$ and A_m are consumption of pump on per hour basis, number of PVTFPCs, solar flux impinging on NPVTFPC and module area respectively. Hourly electrical exergy ($\dot{\mathrm{E}}\mathrm{x}_e(t)$) can be computed using Eq. (17). The value of radiation falling on collector and electrical energy/exergy is considered as zero at night.

4.4. Overall exergy efficacy

The value of overall exergy is computed as addition of thermal exergy and electrical exergy. Overall exergy efficacy on per hour basis for N PVTFPC-DS can be expressed as:

$$\eta_{\text{hourly,overall exergy}} = \frac{\dot{\text{Ex}}_{\text{thermal}}(t) + \left(\dot{\text{Ex}}_e(t) - \dot{P}_u(t)\right)}{0.933 \times \left[\begin{array}{l}\left[\frac{A_b}{2} \times \left(I_{\text{SE}}(t) + I_{\text{SW}}(t)\right)\right] \\ +\left(A_m + A_c\right) \times N \times I(t)\end{array}\right]} \times 100 \quad (24)$$

The value of daily overall exergy efficiency NPVTFPC-DS can be expressed as

$$\eta_{\text{daily,overall exergy}} = \frac{\left[\sum_{t=1}^{t=24} \dot{\text{Ex}}_{\text{thermal}}(t) + \left(\dot{\text{Ex}}_e(t) - \dot{P}_u(t)\right)\right]}{0.933 \times \sum_{t=1}^{24}\left[\begin{array}{l}\left[\frac{A_b}{2} \times \left(I_{\text{SE}}(t) + I_{\text{SW}}(t)\right)\right] \\ +\left(A_m + A_c\right) \times N \times I(t)\end{array}\right]} \times 100 \quad (25)$$

Here, electrical exergy and solar flux values used in Eqs. (24) and (25) are considered as zero for night hours.

4.5. Hourly and daily productivity

The value of productivity on per hour as well as per day basis for NPVTFPC-DS can be computed as [62]:

$$\text{Hourly productivity} = \frac{\left[\text{Hourly yield} \times (\text{SP})_w\right]}{\text{Hourly cost} + \left(\text{Hourly pump work} \times (\text{SP})_e\right)} \times 100 \quad (26)$$

$$\text{Daily productivity} = \frac{\left[\text{Daily yield} \times (\text{SP})_w\right]}{\text{Daily cost} + \left(\text{Daily pump work} \times (\text{SP})_e\right)} \times 100 \quad (27)$$

The value of production of fresh water on per hour basis from NPVTFPC-DS has been estimated utilizing Eq. (10). The value of production of fresh water on per day basis from NPVTFPC-DS has been found by summing the value of production of fresh water on hourly basis for 24 h and pump work on per day basis can be computed by summing pump work on per hour basis for 10 h. The value of cost on per day basis has been computed by dividing uniform end-of-year annual cost (UEAC) with 365 d. Further, the cost on per hour basis has been computed by dividing cost on per day basis with 24 h.

Given initial investment of NPVTFPC-DS, value of UEAC can be expressed taking the concept of present value as [60]:

$$\text{UEAC} = \left(\text{PCS} \times \left(\frac{i \times (1+i)^n}{(1+i)^n - 1}\right)\right) + \left(\text{PCS} \times 0.1 \times \left(\frac{i \times (1+i)^n}{(1+i)^n - 1}\right)\right) - \left(\text{SV} \times \left(\frac{i}{(1+i)^n - 1}\right)\right) \quad (28)$$

where PCS, SV, MC, i and n are respectively present cost, salvage value, maintenance cost, rate of interest and life of NPVTFPC-DS.

The value of PCS for 30 y lifetime of NPVTFPC-DS can be evaluated as [60]:

$$P_s = \text{IC} + \text{PC} + \frac{\text{PC}}{(1+i)^{10}} + \frac{\text{PC}}{(1+i)^{20}} \quad (29)$$

where IC is initial cost of system. PC is the cost of pump including direct current motor. The life of pump has been used as 10 y [14]. Here, it has also been assumed that the value of PC at the time of procuring is same as the present cost if salvage value of pump is adjusted against inflation. The value of IC for NPVTFPC-DS can be calculated as:

$$\text{IC} = C_{\text{DS}} + C_{\text{NPVTFPC}} + C_{\text{man}} \quad (30)$$

where C_{man} represents the cost of manufacturing the system including cost of piping and labor. C_{DS} stands for the cost of DS and C_{NPVTFPC} stands for the cost of N alike PVTFPCs.

The value of UEAC can be calculated using Eq. (28) for different values of N and the annual revenue obtained after selling the potable water can be estimated. Using these two values, one can evaluate productivity.

5. Methodology

The methodology followed for the computation of parameters of NPVTFPC-DS can be stated as follows:

5.1. Step I

The value of solar flux on the flat (horizontal) surface as well as surrounding temperature is taken from Indian Metrological Department, Pune, India. The formula presented by Liu and Jordan is used to compute the value of solar flux for the surface at an angle with horizontal surface at 30° north latitude with the help of MATLAB.

5.2. Step II

The parameters namely T_{foN} and $\dot{Q}_{\text{uN}}(t)$ have been computed using Eqs. (2) and (3) respectively followed by the computation of water temperature, temperatures of glass at outer and inner sides and production of fresh water on per hour basis for NPVTFPC-DS with the help of Eqs. (5)–(8).

5.3. Step III

The exergy output for NPVTFPCs and NPVTFPC-DS has been evaluated using Eqs. (15) and (16) respectively. The electrical exergy for NPVTFPC-DS has been computed using Eq. (17).

5.4. Step IV

The hourly thermal efficacy, daily thermal efficacy, hourly exergy efficacy, daily exergy efficacy, hourly electrical exergy efficacy, daily electrical exergy efficacy, hourly overall exergy efficacy, daily overall exergy efficacy at different water depths for NPVTFPC-DS have been evaluated using Eqs. (18)–(25) respectively. They have been evaluated for different water depth and compared. The average daily

efficiencies have been computed considering two months namely June (summer) and January (winter) at different water depths to assess the effect of dissimilarity of water depth on the performance of NPVTFPC-DS.

5.5. Step V

The hourly and daily productivity at different water depth for NPVTFPC-DS have been obtained using Eqs. (26) and (27) respectively. The average value of productivity on per day basis has been evaluated considering two months namely June (summer) and January (winter) at different water depths to assess the dissimilarity of water depth on the performance of NPVTFPC-DS.

To understand the methodology followed to compute efficiencies and productivity for NPVTFPC-DS in a better way, the flow chart has been drawn and it is depicted as Fig. 2.

6. Results and discussion

The code for computation of various required parameter is written in MATLAB. All required input data like solar flux, surrounding temperature and velocity of air blow are provided to MATLAB. All required equations are also fed to MATLAB. The value of solar flux on flat (horizontal) surface and value of surrounding temperature is depicted in Fig. 3. Values of output received from MATLAB after running the code is depicted in Figs. 4–28.

The dissimilarity of T_{foN} with N for considered value of $\dot{m}_f$ for an archetypal day of June has been depicted as Fig. 4. Fig. 5 depicts the same for an archetypal day

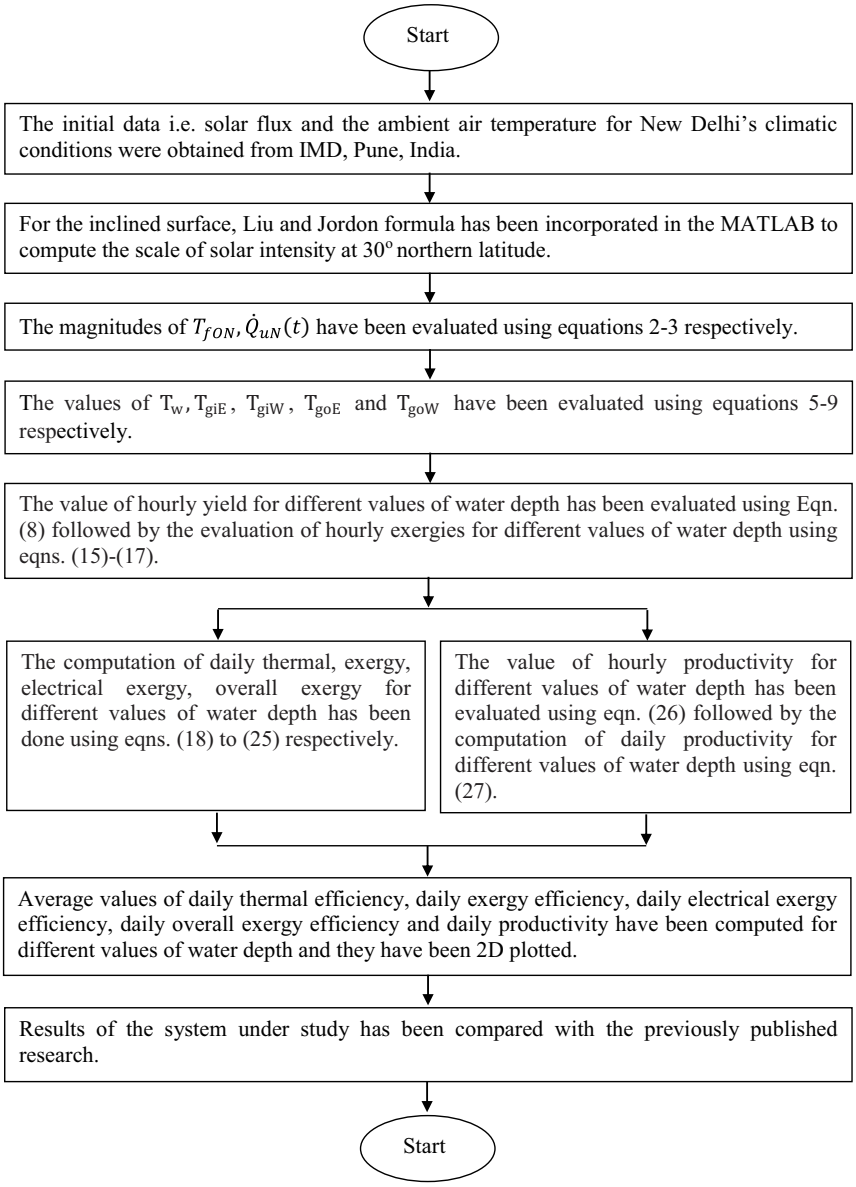

Fig. 2. Methodology for the computation of efficiencies and productivity of NPVTFPC-DS.

of January. One can observe from Figs. 4 and 5 that the value of $\dot{m}_f$ beyond 0.03 kg/s does not result in appreciable increase in heat gain as curves for T_{foN} beyond $\dot{m}_f$ = 0.03 kg/s come very close to each other. The value of heat gain by N alike PVTFPCs depends on the value of $\dot{m}_f$ and ΔT (difference of temperatures between exit of Nth PVTFPC and inlet of first PVTFPC). So, the increased value of heat gain will be obtained at enhanced value of $\dot{m}_f$; however, enhancement in $\dot{m}_f$ values diminish the value of ΔT as diminished values of T_{foN} are obtained at increased value of $\dot{m}_f$ due to less contact time available for fluid for heat absorption. So, the optimum value of $\dot{m}_f$ can be considered as 0.03 kg/s. At this value of $\dot{m}_f$, value of N cannot be taken more than 11 because value of T_{foN} beyond eleven results in the value of T_{foN} more than 100°C and the thermal model will no longer be valid. So, the optimum value of N can be taken as eleven.

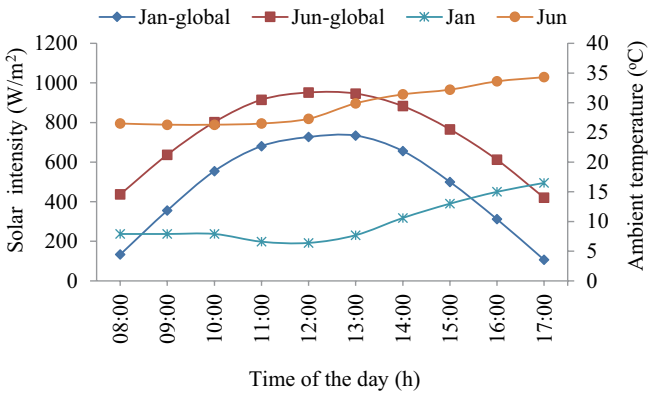

Fig. 3. Hourly dissimilarity of solar intensity on horizontal surface and ambient air temperature.

Fig. 6 depicts the dissimilarity of various temperatures for NPVTFPC-DS for typical day of June. Fig. 7 depicts the similar dissimilarity for typical day of January. One can observe from Figs. 6 and 7 that the value of T_{foN} is highest as expected because heated water from Nth collector is allowed to enter basin. Values of T_{foN} and T_w are highest at 14:00 h because the value of solar flux is highest at 13:00 h and system takes some time to enhance the temperature of water after receiving solar energy due to time

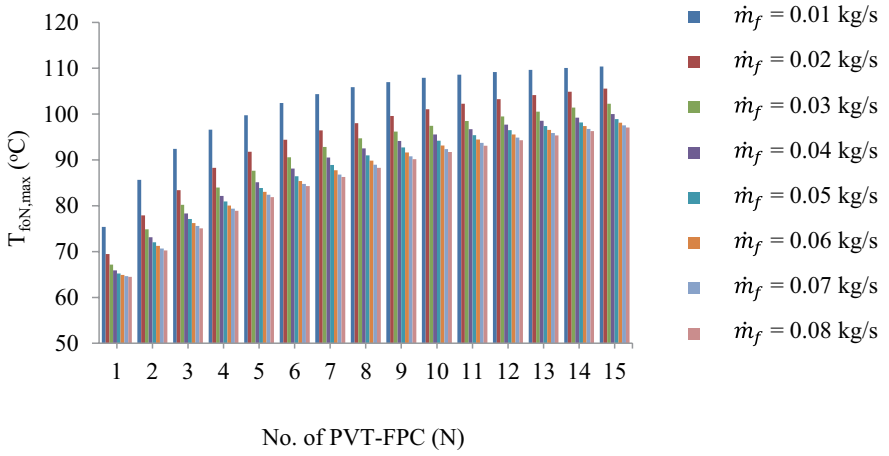

Fig. 4. Variation of maximum temperature of NPVTFPC-DS for an archetypal day of June.

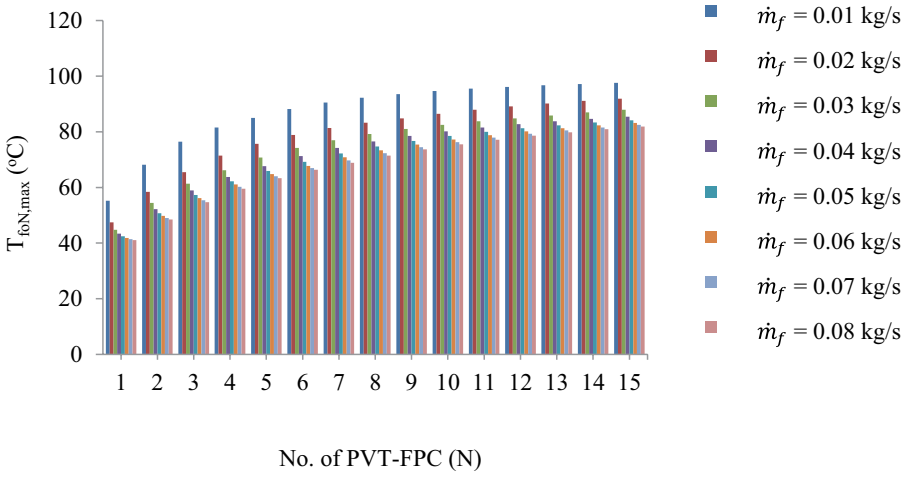

Fig. 5. Variation of maximum temperature NPVTFPC-DS for an archetypal day January.

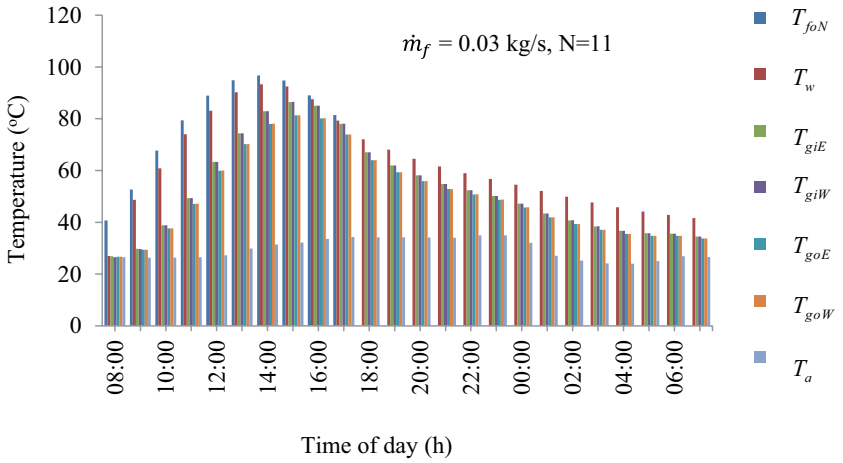

Fig. 6. Hourly variation of various temperature NPVTFPC-DS for an archetypal day of June.

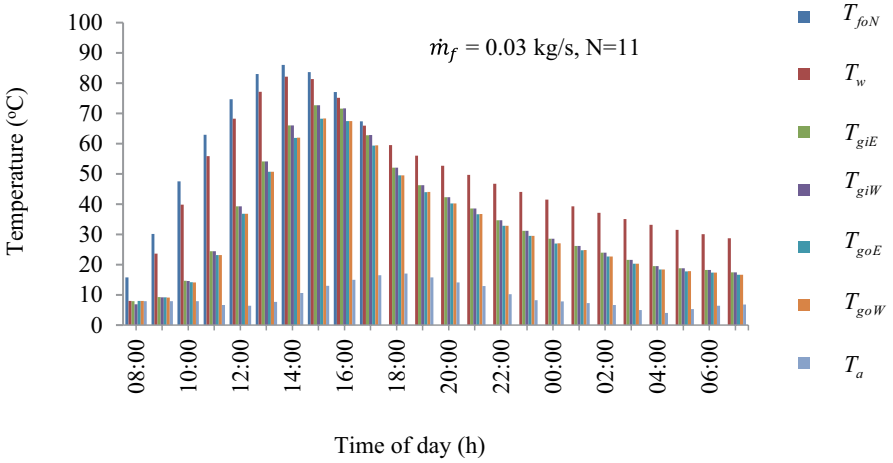

Fig. 7. Hourly variation of various temperature of NPVTFPC-DS for an archetypal day of January.

lag. The dissimilarity of heat transfer coefficients (HTCs) at selected values of $\dot{m}_f$ and N as 0.03 kg/s and eleven for NPVTFPC-DS for an archetypal day of June has been depicted in Fig. 8. Similarly, Fig. 9 depicts the dissimilarity of HTCs for an archetypal day of January. It is observed from Figs. 8 and 9 that the evaporative HTC is highest and this HTC is responsible for the production of fresh water from NPVTFPC-DS. Convective and radiative HTCs are very small as compared to evaporative HTC and convective as well as radiative HTC are responsible for the loss of heat by convection and radiation heat loss phenomena.

The dissimilarity of daily yield and daily yield per unit area with $\dot{m}_f$ for NPVTFPC-DS has been depicted as Fig. 10. One can observe from Fig. 10 that value of freshwater production on per day basis diminishes with the increase in the value of $\dot{m}_f$ because actual heat gain by NPVTFPCs diminishes as the value of $\dot{m}_f$ is enhanced because fluid flowing through tubes of collector does not get sufficient time to absorb solar energy falling on the collector. Fig. 11 depicts the dissimilarity of daily yield and daily yield per unit area with N for NPVTFPC-DS for archetypal days of June and January. It is observed from Fig. 11 that the value of freshwater production on per hour basis is higher in June than the corresponding value in January due to similar trend in solar flux falling on the surface of the system. It is further observed that the value of freshwater production on per day basis enhances with the enhancement in the value of N because increase in N results in more heat collection area and an enhanced value of heat is supplied to basin at increased value of N. Also, increase in daily yield beyond N = 11 is not significant because of the similar trend in actual heat gain by collectors. One can also observe from Fig. 11 that the value of daily yield per unit area first increases and then decreases. It happens because initially increase in daily yield is higher that the increase in area of the system due to increased number of collectors. After certain value of area of the system, daily yield per unit area decreases which occurs because increase in daily yield is less than the increase in area of the system due to increased number of collectors.

The dissimilarity of daily yield with water depth for NPVTFPC-DS for archetypal days of June and January is

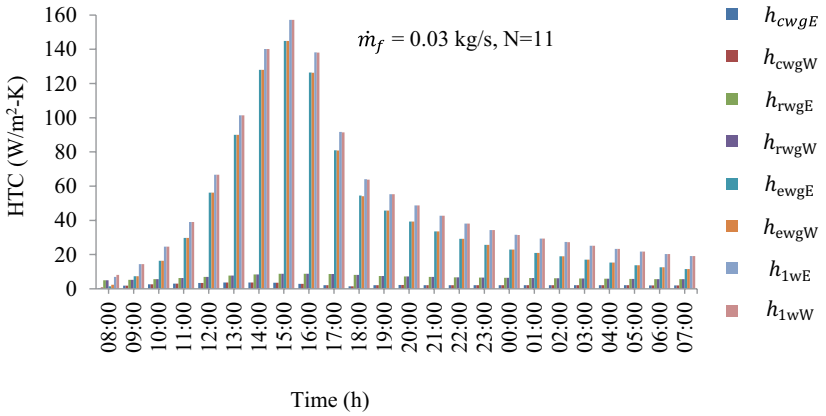

Fig. 8. Hourly variation of heat transfer coefficient (HTC) of NPVTFPC-DS for an archetypal day of June.

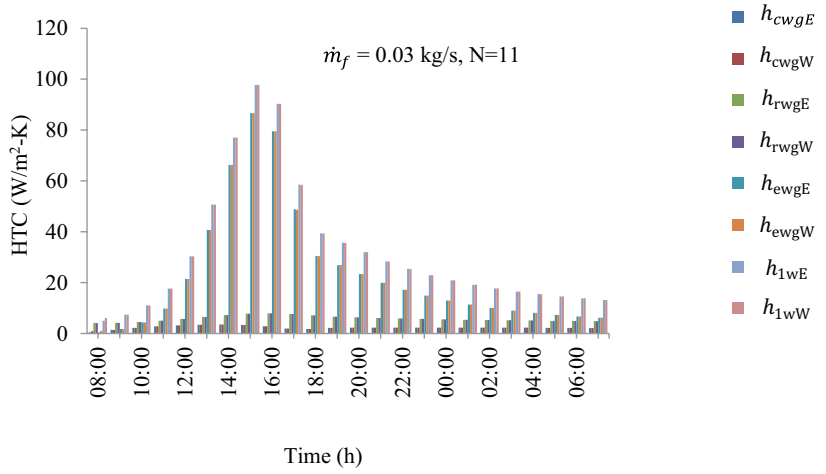

Fig. 9. Hourly variation of heat transfer coefficient (HTC) of NPVTFPC-DS for an archetypal day of January.

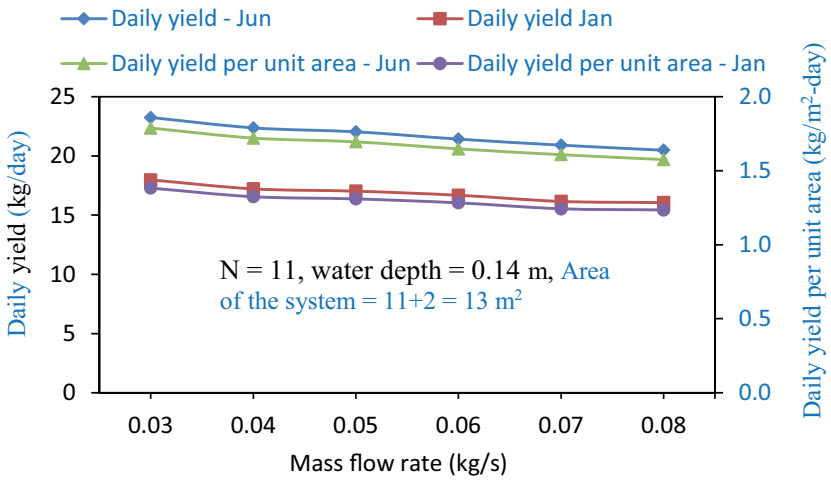

Fig. 10. Dissimilarity of daily yield with $\dot{m}_f$ of NPVTFPC-DS for an archetypal day of June and January.

shown in Fig. 12. One can observe from Fig. 12 that value of freshwater production on per day basis increases with the enhancement in the value of water depth. It happens because increase in freshwater production at night with the enhancement in water depth overcomes the decrease in yield due to water depth in daytime and hence freshwater production on per day basis enhances with the enhancement in the value of water depth. Further, yield

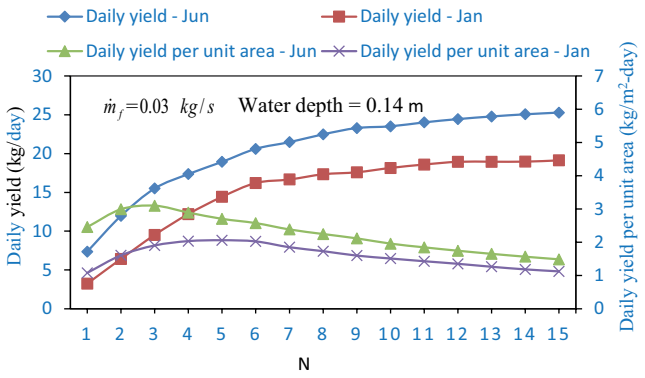

Fig. 11. Dissimilarity of daily yield of NPVTFPC-DS for an archetypal day of June and January.

increases at night with the increase in water depth because of the utilization of stored sensible heat during daytime. The increase in daily yield beyond water depth of 0.70 m is not significant and hence the optimum value of water depth can be considered as 0.70 m; however, this value of water depth is very high and further investigation of set up is required from strength viewpoint. The value of daily yield for NPVTFPC-DS is higher for June than January at all values of water depth because the value of solar flux falling on the surface of system is higher for June than the value of solar flux in January. The dissimilarity of cell temperature and module efficiency for NPVTFPC-DS is depicted as Fig. 13. It is observed from Fig. 13 that the value of cell temperature first increases and then decreases due to similar variation in solar flux falling on the surface of PVT. A reverse trend has been observed in module efficiency. At higher values of cell temperatures, the values of module efficiencies are lower due to increased number of collisions among free electrons at increased values of cell temperature.

The dissimilarity of thermal efficiency on per hour basis of NPVTFPC-DS at optimum values of $\dot{m}_f$ and N for an archetypal day of June and January months is depicted as Figs. 14 and 15 in that order. One can observe from Figs. 14 and 15 that the value of thermal efficiency on per hour basis for NPVTFPC-DS diminishes with the enhancement in the value of water depth as per the expectation. It has been found to occur due to diminished values of water mass temperature in the basin at increased values of water depth. Also, the difference in temperatures of water in basin and inside surface of glass becomes lower at increased depth of water. These two factors are responsible for lower production of fresh water at higher water depth in the basin during sunshine hours and hence lower thermal efficiency is obtained at increased water depth.

The dissimilarity of average values of thermal efficiency for NPVTFPC-DS and NPVTFPC-SS at selected values of $\dot{m}_f$ and N on per day basis is depicted as Fig. 16. One can observe from Fig. 16 that average value of thermal efficiency on per day basis for NPVTFPC-DS/NPVTFPC-SS enhances firstly as depth of water in basin increases and then average values of thermal efficiency on per day basis for NPVTFPC-DS/NPVTFPC-SS becomes more or less constant. It happens because further increase in production of fresh water does not take place due to large mass of water which will not get further heated. The optimum value of average thermal efficiency is thus obtained at water depth of 0.70 m. The average value of daily thermal efficiency has been found to increase initially due to increased value of water mass at night due to sensible heat storage by water mass during sunshine hours. The enhancement in freshwater production at night overcome the diminished production of fresh water in daytime which results in increased value of freshwater production at higher water depth and hence thermal efficiency increases initially with the enhancement in value of water depth. Further, one can observe from Fig. 16 that the mean value of daily thermal efficiency for NPVTFPC-DS is higher if water depth is less than 0.18 m and vice versa. It happens because average daily thermal efficiency depends on average yield, solar energy falling on solar still and heat gain.

The dissimilarity of exergy efficacy on per hour basis NPVTFPC-DS at optimum values of $\dot{m}_f$ and N for an archetypal day of June and January has been depicted as Figs. 17

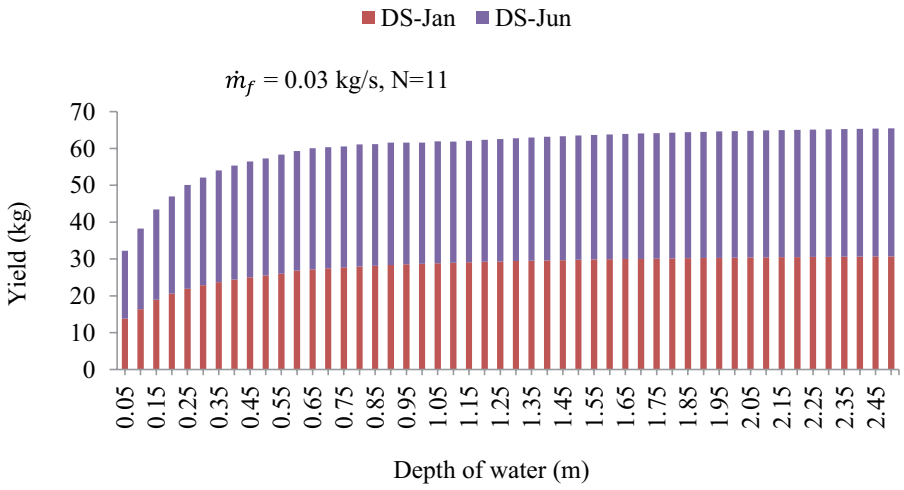

Fig. 12. Variation of yield with water depth of NPVTFPC-DS for an archetypal day of June and January.

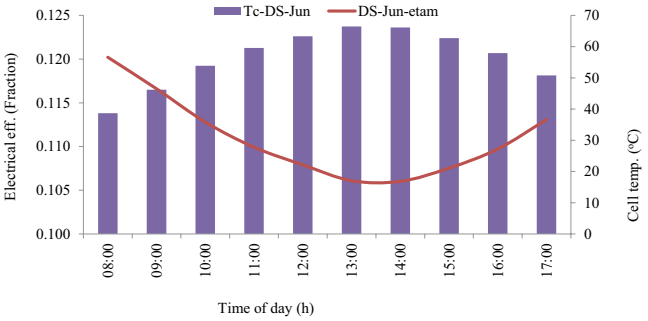

Fig. 13. Dissimilarity of electrical efficiency and average cell temperature for PVT for a typical day in the month of June.

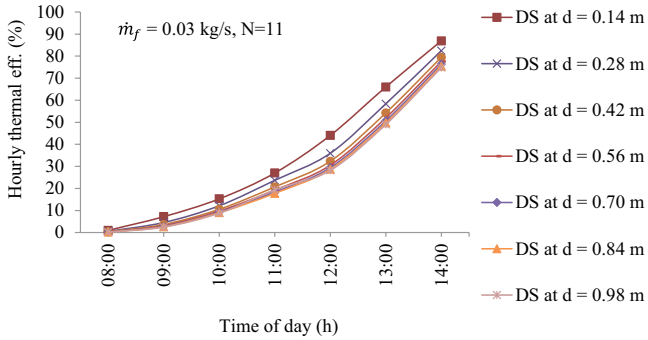

Fig. 14. Dissimilarity of hourly thermal efficiency with water depth for NPVTFPC-DS for an archetypal day of June.

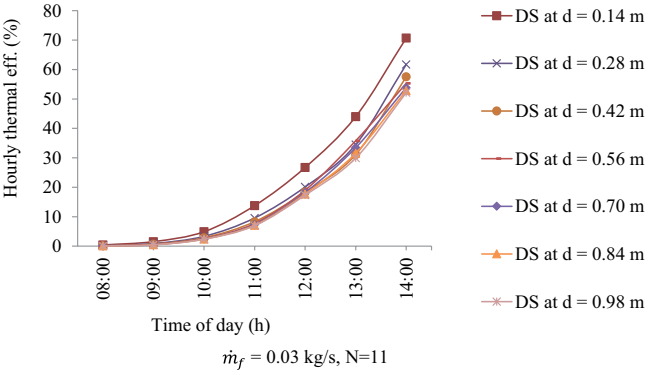

Fig. 15. Dissimilarity of hourly thermal efficiency with water depth for NPVTFPC-DS for an archetypal day of January.

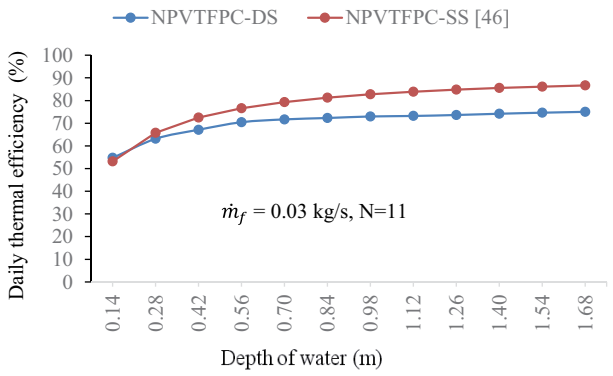

Fig. 16. Comparison of dissimilarity of average daily thermal efficiency with depth of water for NPVTFPC-DS and NPVTFPC-SS.

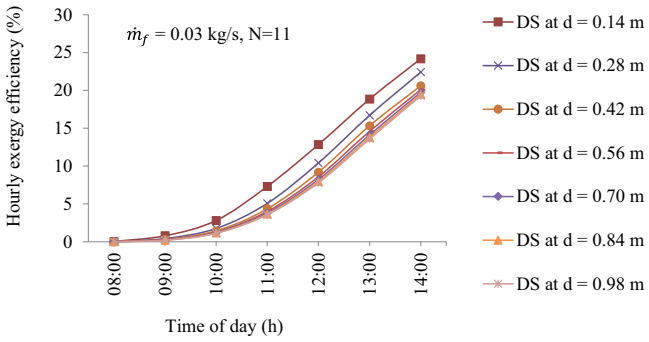

Fig. 17. Dissimilarity of hourly exergy efficiency with water depth for NPVTFPC-DS for an archetypal day of June.

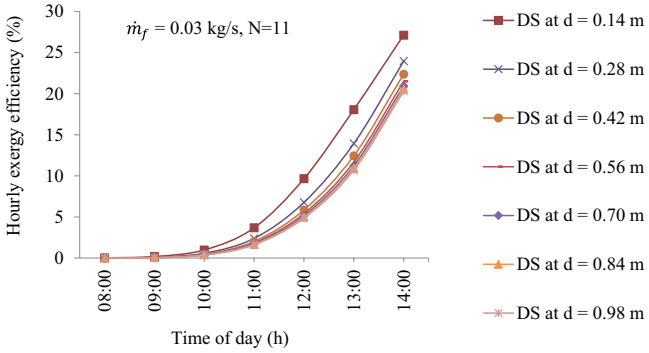

Fig. 18. Dissimilarity of hourly exergy efficiency with water depth for NPVTFPC-DS for an archetypal day of January.

and 18 in that order. One can observe from Figs. 17 and 18 that the hourly exergy efficiency of NPVTFPC-DS diminishes with the enhancement in water depth for the daytime as expected. The reason being that water mass temperature in basin diminishes as the values of water depth enhances. Further, the difference in temperatures of water in basin and inside surface of glass becomes lower at increased depth of water. These two factors are responsible for lower exergy gain by NPVTFPC-DS during sunshine hours (daytime). Also, exergy output is the function of temperature, and it is considered as high-grade energy which basically represents the quality of energy. So, lower exergy is gained by NPVTFPC-DS at lower temperature because of higher loss.

The dissimilarity of average exergy efficiency on per day basis with water depth for NPVTFPC-DS and NPVTFPC-SS at optimum values of $\dot{m}_f$ and N is depicted as Fig. 19. It has been observed from Fig. 19 that values of average exergy efficiency on per day basis for NPVTFPC-DS/NPVTFPC-SS first increases and then become approximately constant. It has been found to occur because further increase in exergy does not take place due to large

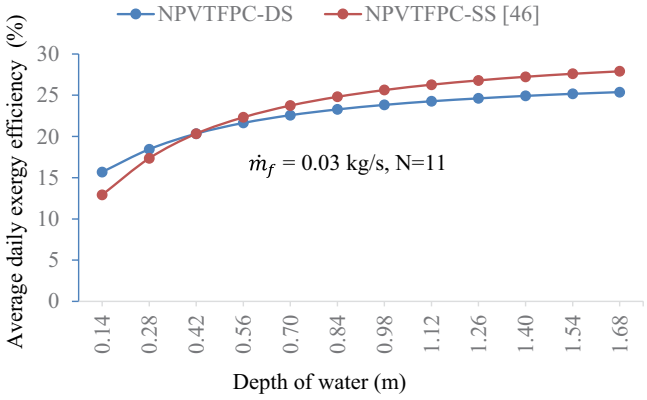

Fig. 19. Comparison of dissimilarity of average daily exergy efficiency with depth of water for NPVTFPC-DS and NPVTF-PC-SS.

mass of water which will not get further heated. Thus, the optimum value of exergy efficiency for the system has been found as 0.70 m. Further, the value of average daily exergy efficiency is higher for NPVTFPC-DS if water depth is less than 0.42 m and NPVTFPC-SS performs better than NPVT-FPC-DS if water depth is more than 0.42 m. It happens because average daily exergy efficiency depends on average exergy gain, sun exergy entering the basin through glass cover and exergy gain of PVTFPC entering the basin. At lower water depth, rise in water temperature is more in the case of NPVTFPC-DS because moderate intensity exists for a longer period in the case of double slope, whereas in the case of single slope, higher intensity exists for a shorter period. At higher depth, moderate intensity for a longer period which exists in the case of double slope is not sufficient to rise the water temperature due to heat capacity of water. However, higher intensity for a shorter period which exists in the case of single slope is capable of raising the water temperature higher than NPVTFPC-DS.

The dissimilarity of hourly electrical efficiency with water depth for NPVTFPC-DS for archetypal days of June and January has been depicted as Figs. 20 and 21 in that order. It is observed from Figs. 20 and 21 that electrical exergy efficacy on per hour basis first enhances and then diminishes. The enhancement in the value of electrical exergy efficacy on per hour basis is obtained because of the enhancement in value of solar flux. However, it again diminishes because there is an increase in temperature as higher solar intensity enhances and an increased number of collisions among electrons is obtained at increased temperatures which results in diminished production of current. Hence, diminished values of electrical exergy efficacy are obtained. Fig. 22 depicts the dissimilarity of average electrical exergy efficacy on per day basis for NPVTFPC-DS/NPVTFPC-SS. The value of average electrical exergy efficacy on per day basis is approximately equal at all values of water depth because PV module temperature remains approximately same for all values of water depth.

The dissimilarity of hourly overall exergy efficacy with depth of water for NPVTFPC-DS at optimum values of N and $\dot{m}_f$ for archetypal days of June and January has been depicted as Figs. 23 and 24 in that order. It is

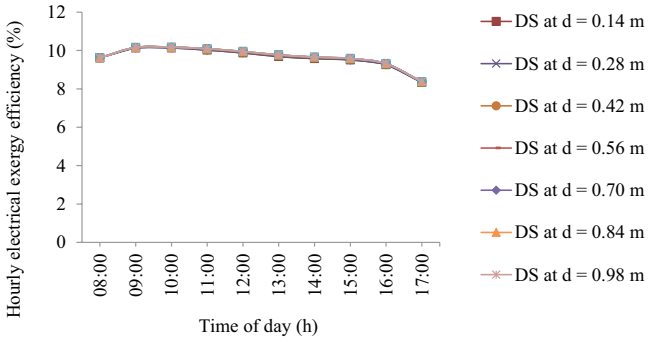

Fig. 20. Dissimilarity of hourly electrical efficiency with water depth for NPVTFPC-DS for an archetypal day of June.

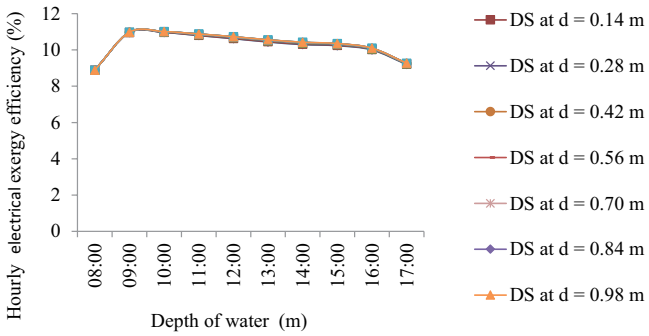

Fig. 21. Dissimilarity of hourly electrical efficiency with water depth for NPVTFPC-DS for an archetypal day of January.

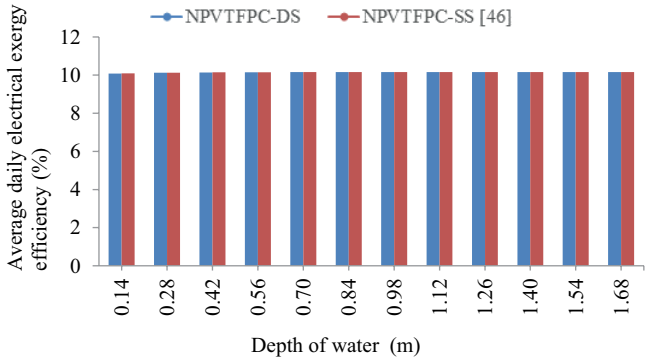

Fig. 22. Comparison of dissimilarity of average daily electrical exergy efficiency with depth of water for NPVTFPC-DS and NPVTFPC-SS.

observed from Figs. 23 and 24 that the value of hourly overall exergy for NPVTFPC-DS diminishes with the enhancement in value of water depth during daytime because augmentation in water temperature is smaller at increased depth of water. The dissimilarity of value of average overall exergy efficacy on per day basis with water depth for NPVTFPC-DS/NVTFPC-SS has been depicted in Fig. 25. It is observed from Fig. 25 that the value of average daily exergy efficacy first enhances for NPVTFPC-DS/NPVTFPC-SS up to water depth of 0.7 m. Then, the value of average daily exergy efficacy becomes almost steady. It represents that the optimal value of water depth for

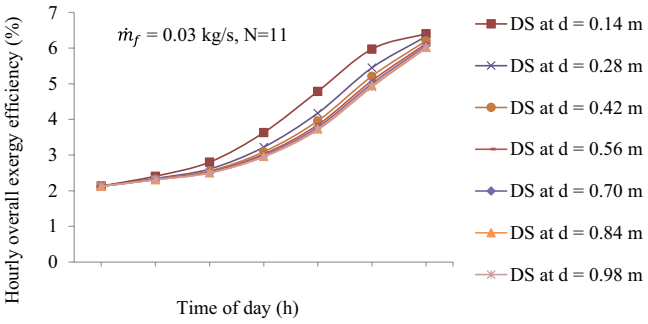

Fig. 23. Dissimilarity of hourly overall exergy efficiency with water depth NPVTFPC-DS for an archetypal day of June.

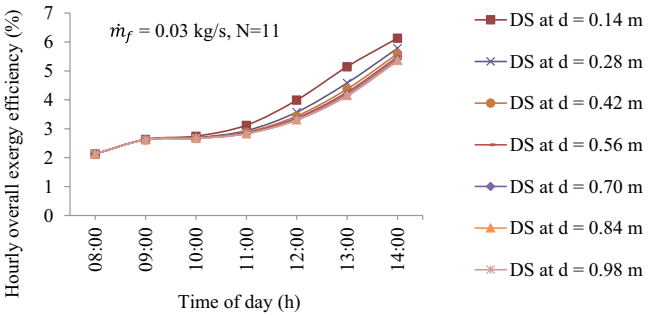

Fig. 24. Dissimilarity of hourly overall exergy efficiency with water depth for NPVTFPC-DS for an archetypal day of January.

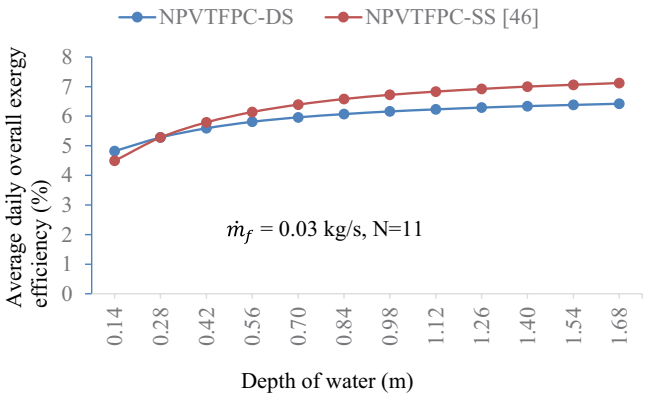

Fig. 25. Comparison of dissimilarity of average overall daily exergy efficiency with water depth for NPVTFPC-DS and NPVTFPC-SS.

NPVTFPC-DS/NPVTFPC-SS is 0.7 m from overall exergy efficacy viewpoint. However, system tends to be massive at such depth of water. Hence, further study is required to operate at this water depth. It happens because there is not much rise in water temperature beyond 0.7 m water depth as the mass of water in the basin becomes large.

It has also been observed from Fig. 25 that NPVTFPC-DS performs better than NPVTFPC-SS if water depth is less than 0.28 m and vice versa on the basis of mean daily overall exergy efficiency. It happens because average daily overall exergy efficiency depends on average exergy gain, sun exergy entering the basin through glass cover, exergy gain of PVT-FPC entering the basin and electrical exergy generated by PVT. The electrical exergy is almost same in both cases. However, thermal exergy is different. At lower water depth, rise in water temperature is more in the case of NPVTFPC-DS because moderate intensity exists for a longer period in the case of NPVTFPC-DS, whereas in the case of NPVTFPC-SS, higher intensity exists for a shorter period. At higher depth, moderate intensity for a longer period which exists in the case of NPVTFPC-DS is not sufficient to raise water temperature due to heat capacity of water. However, higher intensity for a shorter period which exists in the case of NPVTFPC-SS is capable of raising the water temperature higher than NPVT-FPC-DS.

The dissimilarity of productivity on per hour basis of NPVTFPC-DS at optimum values of $\dot{m}_f$ and N for archetypal days of June and January is depicted as Figs. 26 and 27 in that order. Values of interest rate, life span of NPVTFPC-DS and the price of fresh water on per kg basis produced from NPVTFPC-DS have been considered as 5%, 50 y and ₹5 respectively for the computation of values of uniform end-of-year annual cost for NPVTFPC-DS/NPVTFPC-SS. The cost of different components of NPVTFPC-DS is depicted as Table 2. The value of UEAC has been evaluated using Eq. (28) and presented in Table 3. One can observe that the value of productivity on per hour basis for NPVTFPC-DS diminishes with the increase in water depth during daytime. Further, during night-time, value of productivity on per hour basis for NPVTFPC-DS increases with increase in water depth. It occurs because the production of fresh water from NPVTFPC-DS diminishes as depth of water enhances during daytime due to diminished rise in temperature which results in diminished difference of temperatures between water surface and inside surface of glass cover. During night-time, an opposite phenomenon is observed because the production of fresh water from NPVTFPC-DS enhances because the enhanced sensible heat gets stored by water mass in the basin during daytime at increased water depth and this increased stored sensible heat is utilized at night-time.

Fig. 28 depicts the dissimilarity of average productivity on per day basis with depth of water at optimum values of $\dot{m}_f$ and N for NPVTFPC-DS and NPVTFPC-SS. The value of average daily productivity for NPVTFPC-DS/NPVTFPC-SS first increases till 0.70 m water depth and then becomes almost constant. It happens because average daily productivity depends on average daily yield and daily cost. The optimum value of productivity is obtained corresponding to 0.70 m water depth. It is also observed that NPVTFPC-DS performs better than NPVTFPC-SS on the basis of average daily productivity if water depth is less than 0.18 m and NPVTFPC-SS performs better than NPVTFPC-DS on the basis of average daily productivity if water depth is more than 0.18 m. Further, average daily productivity for both cases is almost constant beyond 0.70 m depth of water. It means 0.70 m is the optimum depth for both cases based on average daily productivity. It happens because both yield and electricity gain remain almost constant beyond 0.70 m water depth.

Table 4 depicts the comparison of NPVTFPC-DS with similar set up available in the literature based on different

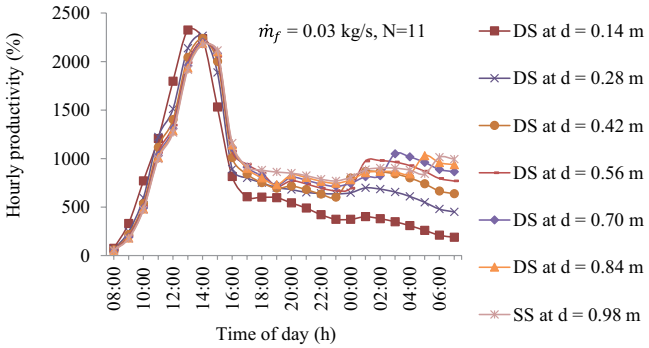

Fig. 26. Dissimilarity of hourly productivity with depth of water of NPVTFPC-DS for an archetypal day of June.

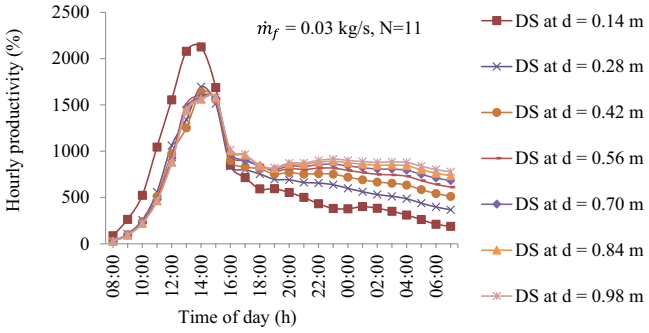

Fig. 27. Dissimilarity of hourly productivity with depth of water for NPVTFPC-DS for an archetypal day of January.

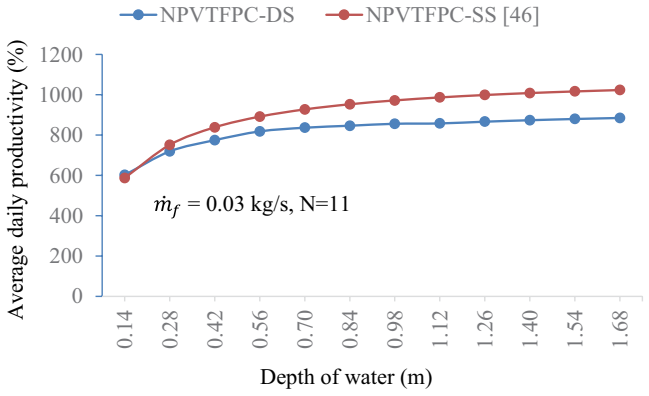

Fig. 28. Comparison of dissimilarity of average daily productivity with depth of water for NPVTFPC-DS and NPVTFPC-SS.

average daily efficacies and annual productivity. The rate of interest and life span has been taken as 5% and 50 y, respectively. It has been observed that the value of average daily thermal efficiency, average daily exergy efficiency, average daily overall exergy efficiency and average daily productivity of NPVTFPC-DS is higher by 2.89%, 17.65%, 6.85% and 2.42% respectively than NPVTFPC-SS at 0.14 m water depth and optimum values of N and $\dot{m}_f$. The better performance of NPVTFPC-DS is obtained due to better distribution of solar flux which results in higher production of fresh water as well as exergy. It is also observed that the value of average electrical exergy for NPVTFPC-DS is approximately same as the average electrical exergy efficiency for NPVTFPC-DS at 0.14 m water depth and optimum values of N and $\dot{m}_f$ due to approximately same solar cell temperatures in both cases. Values of average daily efficiencies and annual productivity are lower for passive solar still because yield is lower due to the absence of collectors.

7. Conclusions

The theoretical analysis of NPVTFPC-DS has been carried out to assess the effect of water depth on thermal efficiency, exergy efficiency, electrical exergy efficiency, overall exergy efficiency and productivity. Results of NPVTFPC-DS has been compared with NPVTFPC-SS published earlier. Based on the current research, the conclusions have been drawn as follows:

- Hourly thermal, exergy, electrical exergy and overall exergy efficiencies of NPVTFPC-DS have been found to diminish with increase in water depth during sunshine hours.
- The average daily thermal, exergy and overall exergy efficiencies first rise and then become almost constant beyond 0.70 m; whereas, the value of daily electrical exergy efficiency has been found to be same at all values of water depth.
- The value of hourly productivity of NPVTFPC-DS diminishes with the increase in water depth during sunshine hours (day). However, it has been found to increase with the increase in depth of water during off sunshine hours (night). The average hourly productivity also first increase till 0.70 m and then becomes almost constant and hence water depth of 0.70 m has been found to be optimum from productivity viewpoint. However, the system becomes bulky at water depth of 0.70 m and hence further study is required from strength viewpoint.

Table 2
Capital investments for solar energy operated water purifier of double slope type coupled to N alike ETCs

S. No.	Parameter	Cost (₹) of DS
1	Cost of solar still	19,183
2	Cost of PVTFPC	93,500
3	Cost of motor and pump	1,000
4	Fabrication cost	6,000
5	Salvage value of the system after 50 y, if inflation remains @ 4% in India, [using present value of scrap material sold in Indian market]	80,080

Table 3
Value of UEAC solar energy operated water purifier of double slope type coupled to N alike ETCs (N = 11)

n	i	P_s	M	S_s	$F_{CR,i,n}$	$F_{SR,i,n}$	UEAC
Y	%	₹	@ 10%	₹	Fraction	Fraction	₹
50	2	122,181.28	12,218.13	80,080	0.03182	0.01182	3,330.04
50	5	121,047.23	12,104.72	80,080	0.05478	0.00478	6,911.28
50	10	120,296.59	12,029.66	80,080	0.10086	0.00086	13,277.56

Table 4
Comparison of NPVTFPC-DS with similar set up on the basis of various efficiencies and annual productivity

Parameter → System ↓	Average daily efficiency				Daily productivity
	Thermal	Exergy exergy	Electrical exergy	Overall exergy	
	(%)	(%)	(%)	(%)	(%)
NPVTFPC-DS	54.71	15.69	10.09	4.82	601.92
NPVTFPC-SS [46]	53.13	12.92	10.08	4.49	587.33
Single slope passive solar still [63]	45.03	4.49	–	–	555.55
Double slope passive solar still [63]	42.67	4.35	–	–	584.11
NPVTFPC-SS for N = 2 [64]	11.6	3.93	7.24	5.71	254.06

- Values of average daily thermal, exergy, overall exergy efficiencies and average daily productivity for NPVTFPC-DS are better than the corresponding values for similar set up of single slope type at 0.14 m water depth. However, average daily electrical exergy efficiency values are same for both the cases.
- The mean value of daily thermal efficiency, daily exergy efficiency, daily overall exergy efficiency and daily productivity is higher respectively for NPVTFPC-DS than NPVTFPC-SS if water depth is less than 0.18, 0.42, 0.28 and 0.18 m and vice-versa.

9. Recommendations

The outcome of this research will help the designer and installer of solar energy operated water purifier of double slope type working in active mode for selecting the water depth from thermal efficacy, exergy efficacy, electrical exergy efficacy, overall exergy efficacy and productivity viewpoints under selected values of $\dot{m}_f$ and N. The solar energy operated water purifier of double slope type working in active mode has not been tested experimentally. So, authors recommend its experimental validation before the actual installation as solar energy operated water purifier plant. The optimal values of water depth for solar energy operated water purifier coupled to N alike PVTFPCs has been identified as 0.70 m from efficacies and productivity viewpoints at $\dot{m}_f$ = 0.03 kg/s and N = 11. The optimal values identified with this analysis are for the location of New Delhi, a similar analysis can be used to provide new values that will be optimal for different location and weather conditions. The authors plan to extend this research to include geographic and weather variations in future research.

Symbols

C — Specific heat capacity, J/kg-K
C_{man} — Cost of manufacturing the system including cost of piping and labor, ₹
F' — Collector efficiency factor, dimensionless
h_{cwgE} — Convective heat transfer coefficient from water to inner surface of glass cover facing east, W/m²-K
h_{cwgW} — Convective heat transfer coefficient from water to inner surface of glass cover facing west, W/m²-K
h_{ewgW} — Evaporative heat transfer coefficient from water to inner surface of glass cover facing west, W/m²-K
h_{ewgE} — Evaporative heat transfer coefficient from water to inner surface of glass cover facing east, W/m²-K
h_{ba} — Heat transfer coefficient from blackened surface to ambient, W/m²-K
h_{bw} — Heat transfer coefficient from blackened surface to water mass, W/m²-K
h — Heat transfer coefficient, W/m²-K
h_{rwgE} — Radiative heat transfer coefficient from water surface to inner surface of glass cover facing east, W/m²-K
h_{rwgW} — Radiative heat transfer coefficient from water surface to inner surface of glass cover facing west, W/m²-K
h_r — Radiative heat transfer coefficient, W/m²-K
h_{1wE} — Total heat transfer coefficient from water surface to inner surface of glass cover facing east, W/m²-K

h_{1wW} — Total heat transfer coefficient from water surface to inner surface of glass cover facing west, W/m²-K
h_{1gE} — Total heat transfer coefficient from water surface to inner glass cover facing east, W/m²-K
h_{1gW} — Total heat transfer coefficient from water surface to inner glass cover facing west, W/m²-K
$I(t)$ — Solar intensity on collector, W/m²
$I_S(t)$ — Solar intensity on NETC-SEOWPDS
i — Rate of interest, %
K — Thermal conductivity, W/m-K
L_g — Thickness of glass, m
L — Latent heat, J/kg
L' — Length, m
$\dot{m}_f$ — Mass flow rate of fuid/water, kg/s
N — Number of collectors
n — Life of NPVTFPC-SEODSWP, y
PVT — Photovoltaic thermal
PF_c — Penalty factor due to the glass covers for the glazed portion
PF_1 — Penalty factor first, dimensionless
PF_2 — Penalty factor second, dimensionless
$\dot{Q}_{uN}$ — Heat gain from N identical series connected PVTFPCs, kWh
r — Radius of copper tube, m
T_{foN} — Outlet water temperature at the end of Nth water collector, °C
$T\alpha$ — Ambient air temperature, °C
t — Time, h
U_L — Overall heat transfer coefficient, W/m²-K
V — Velocity of air, m/s

Subscripts

eff — Effective
ex — Exergy
f — Fluid
in — Incoming
out — Outgoing
w — Water
DS — Double slope solar still
E — East
W — West

Greek

α — Absorptivity (fraction)
η — Efficiency, %
$(\alpha\tau)_{eff}$ — Product of effective absorptivity and transmittivity
σ — Stefan–Boltzmann constant, W/m²-K⁴
τ — Transmittivity
β_c — Packing factor

Abbreviations

UEAC — Uniform end-of-year annual cost, ₹
CRF — Capital recovery factor
CPC — Compound parabolic concentrating collector
ETC — Evacuated tubular collector
FPC — Flat plate collector
HTC — Heat transfer coefficient, W/m²-K
IC — Initial cost of system, ₹
MC — Maintenance cost of NETC-SEOWPDS, ₹
MCF — Maintenance cost factor
NPVTFPCSS — N alike partially covered photovoltaic thermal flat plate collectors integrated SS
NPVTCPCSS — N alike partially covered photovoltaic thermal CPC integrated SS
PCS — Present cost of N-ETC, ₹
PW — Potable water
PC — Cost of pump including direct current motor, ₹
PVT — Photovoltaic thermal
SV — Salvage value of NETC-SEOWPDS, ₹
DS — Double slope solar still
SS — Single slope solar still
SFF — Sinking fund factor

References

[1] S.N. Rai, G.N. Tiwari, Single basin solar still coupled with flat plate collector, Energy Convers. Manage., 23 (1983) 145–149.
[2] G.N. Tiwari, NK. Dhiman, Performance study of a high temperature distillation system, Energy Convers. Manage., 32 (1991) 283–291.
[3] S.A. Lawrence, G.N. Tiwari, Theoretical evaluation of solar distillation under natural circulation with heat exchanger, Energy Convers. Manage., 30 (1990) 205–213.
[4] O.A. Hamadou, K. Abdellatif, Modeling an active solar still for sea water desalination process optimization, Desalination, 354 (2014) 1–8.
[5] C. Tiris, M. Tiris, Y. Erdalli, M. Sohmen, Experimental studies on a solar still coupled with a flat plate collector and a single basin still, Energy Convers. Manage., 39 (1998) 853–856.
[6] O.O. Badran, H.A. Al-Tahaineh, The effect of coupling flat plate collector on the solar still productivity, Desalination, 183 (2004) 137–142.
[7] R. Tripathi, G.N. Tiwari, Effect of water depth on internal heat and mass transfer for active solar distillation, Desalination, 173 (2005) 187–200.
[8] A.A. Badran, A.A. Al-Hallaq, I.A. Eyal Salman, M.Z. Odat, A solar still augmented with a flat-plate collector, Desalination, 172 (2005) 227–234.
[9] A.J.N. Khalifa, A.M. Hamood, On the verification of the effect of water depth on the performance of basin type solar stills, Sol. Energy, 83 (2009) 1312–1321.
[10] H. Taghvaei, H. Taghvaei, J. Khosrow, M.R. Karimi Estahbanati, M. Feilizadeh, M. Feilizadeh, A. Seddigh Ardekani, A thorough investigation of the effects of water depth on the performance of active solar stills, Desalination, 347 (2014) 77–85.
[11] F. Saeedi, F. Sarhaddi, A. Behzadmehr, Optimization of a PV/T (photovoltaic/thermal) active solar still, Energy, 87 (2015) 142–152.
[12] L. Sahota, G.N. Tiwari, Advanced Solar-Distillation Systems: Basic Principles, Thermal Modeling, and Its Application, Springer, Singapore, 2017.
[13] M. Veeramanikandan, T.V. Arjunan, N. Gunasekar, Numerical simulation and experimental validation of a novel sandwich glazed photovoltaic thermal (SGPV/T) water heating system, Energy Sources, Part A, (2021), doi: 10.1080/15567036.2021.1945711.
[14] S. Kumar, A Tiwari, Design, fabrication, and performance of a hybrid photovoltaic/thermal (PVT) active solar still, Energy Convers. Manage., 51 (2010) 1219–1229.
[15] G.N. Tiwari, J.K. Yadav, D.B. Singh, I.M. Al-Helal, A.M. Abdel-Ghany, Exergoeconomic and enviroeconomic analyses of partially covered photovoltaic flat plate collector active solar distillation system, Desalination, 367 (2015) 186–196.

[16] D.B. Singh, J.K. Yadav, V.K. Dwivedi, S. Kumar, G.N. Tiwari, I.M. Al-Helal, Experimental studies of active solar still integrated with two hybrid PVT collectors, Sol. Energy, 30 (2016) 207–223.
[17] M. Feilizadeh, M.R.K. Estahbanati, A. Ahsan, K. Jafarpur, A. Mersaghian, Effects of water and basin depths in single basin solar stills: an experimental and theoretical study, Energy Convers. Manage., 122 (2016) 174–181.
[18] A.E. Kabeel, R. Sathyamurthy, S.W. Sharshir, A. Muthumanokar, H. Panchal, N. Prakash, C. Prasad, S. Nandakumar, M.S. El Kady, Effect of water depth on a novel absorber plate of pyramid solar still coated with TiO_2 nano black paint, J. Cleaner Prod., 213 (2018) 185–191.
[19] A.E. Kabeel, S.W. Sharshir, G.B. Abdelaziz, M.A. Halim, A. Swidan, Improving performance of tubular solar still by controlling the water depth and cover cooling, J. Cleaner Prod., 233 (2019) 848–856.
[20] R.J. Issa, B. Chang, Performance study on evacuated tubular collector coupled solar still in West Texas climate, Int. J. Green Energy, 14 (2018) 793–800.
[21] D.B. Singh, Improving the performance of single slope solar still by including N identical PVT collectors, Appl. Therm. Eng., 131 (2018) 167–179.
[22] D.B Singh, Energy metrics analysis of N identical evacuated tubular collectors integrated single slope solar still, Energy, 148 (2018a) 546–560.
[23] M. Fathy, H. Hassan, M.S. Ahmed, Experimental study on the effect of coupling parabolic trough collector with double slope solar still on its performance, Sol. Energy, 163 (2018) 54–61.
[24] D.B. Singh, G.N. Tiwari, Analytical characteristic equation of N identical evacuated tubular collectors integrated double slope solar still, J. Sol. Energy Eng. Trans. ASME, 135 (2017) 051003 (1–11), doi: 10.1115/1.4036855.
[25] R. Kumar, R. Sharma, D. Kumar, A.R. Singh, D.B. Singh, G.N Tiwari, Characteristic equation development for single-slope solar distiller unit augmented with N identical parabolic concentrator integrated evacuated tubular collectors, J. Sol. Energy Eng. Trans. ASME, 142 (2020) 021011 (1–11), doi: 10.1115/1.4045314.
[26] H. Prasad, P. Kumar, R.K. Yadav, A. Mallick, N. Kumar, D.B. Singh, Sensitivity analysis of N identical partially covered (50%) PVT compound parabolic concentrator collectors integrated double slope solar distiller unit, Desal. Water Treat., 153 (2019) 54–64.
[27] D.B. Singh, N. Kumar, Harender, S. Kumar, S.K. Sharma, A. Mallick, Effect of depth of water on various efficiencies and productivity of N identical partially covered PVT collectors incorporated single slope solar distiller unit, Desal. Water Treat., 138 (2019) 99–112.
[28] D.B. Singh, G. Bansal, H. Prasad, A. Mallick, N. Kumar, S.K. Sharma, Sensitivity analysis of N undistinguishable photovoltaic thermal compound-parabolic-concentrator collectors (partly covered, 50%) integrated single-slope solar distiller unit, J. Sol. Energy Eng. Trans. ASME, 143 (2020) 021003 (1–11), doi: 10.1115/1.4048012.
[29] A.M. Manokar, Y. Taamneh, A.E. Kabeel, W.D. Prince, P. Vijayabalan, D. Balaji, R. Sathyamurthy, S.S. Padmanaba, D. Mageshbabu, Effect of water depth and insulation on the productivity of an acrylic pyramid solar still – an experimental study, Groundwater Sustainable Dev., 10 (2020) 100319, doi: 10.1016/j.gsd.2019.100319.
[30] K.V. Modi, K.H. Nayi, S.S. Sharma, Influence of water mass on the performance of spherical basin solar still integrated with parabolic reflector, Groundwater Sustainable Dev., 10 (2020) 100299, doi: 10.1016/j.gsd.2019.100299.
[31] K.V. Modi, D.L. Shukla, D.B. Ankoliya, A comparative performance study of double basin single slope solar still with and without using nanoparticles, J. Sol. Energy Eng. Trans. ASME, 141 (2019) 031008 (10 pages), doi: 10.1115/1.4041838.
[32] A.E. Kabeel, A.M. Manokar, R. Sathyamurthy, D.P. Winston, S.A. El-Agouz, A.J. Chamkha, A review on different design modifications employed in inclined solar still for enhancing the productivity, J. Sol. Energy Eng. Trans. ASME, 141 (2019) 031007 (10 pages), doi: 10.1115/1.4041547.
[33] P. Pal, R. Dev, Thermal modeling, experimental validation, and comparative analysis of modified solar stills, J. Sol. Energy Eng. Trans. ASME, 141 (2019) 061013 (16 pages), doi: 10.1115/1.4043955.
[34] A.C. Groenewoudt, H.K. Romijn, F. Alkemade, From fake solar to full service: an empirical analysis of the solar home systems market in Uganda, Energy Sustainable Dev., 58 (2020) 100–111.
[35] H. Ye, Y. Zheng, H. Zheng, S. Liang, Sustainable agriculture irrigation system using a novel solar still design with a compound parabolic concentrator reflector, J. Sol. Energy Eng. Trans. ASME, 142 (2020) 031010 (7 pages), doi: 10.1115/1.4045826.
[36] P.M. Sivaram, S.D. Kumar, M. Premalatha, T. Sivasankar, A. Arunagiri, Experimental investigation on airflow and water production in the integrated rooftop solar thermal system, J. Sol. Energy Eng. Trans. ASME, 142 (2020) 031006 (15 pages), doi: 10.1115/1.4045738.
[37] K. Mohammadi, H. Taghvaei, E.G. Rad, Experimental investigation of a double slope active solar still: effect of a new heat exchanger design performance, Appl. Therm. Eng., 180 (2020) 115875, doi: 10.1016/j.applthermaleng.2020.115875.
[38] R. Fallahzadeh, A. Aref, V.M. Avargani, N. Gholamiarjenaki, An experimental investigation on the performance of a new portable active bubble basin solar still, Appl. Therm. Eng., 181 (2020) 115918, doi: 10.1016/j.applthermaleng.2020.115918.
[39] F.A. Essa, M.A. Elaziz, A.H. Elsheikh, An enhanced productivity prediction model of active solar still using artificial neural network and Harris Hawks optimizer, Appl. Therm. Eng., 170 (2020) 115020, doi: 10.1016/j.applthermaleng.2020.115020.
[40] O.D. Maliani, A. Bekkaoui, E.H. Baali, K. Guissi, Y. El Fellah, R. Errais, Investigation on novel design of solar still coupled with two axis solar tracking system, Appl. Therm. Eng., 172 (2020) 115144, doi: 10.1016/j.applthermaleng.2020.115144.
[41] V.S. Gupta, D.B. Singh, S.K. Sharma, N. Kumar, T.S. Bhatti, G.N. Tiwari, Modeling self-sustainable fully-covered photovoltaic thermal-compound parabolic concentrators connected to double slope solar distiller, Desal. Water Treat., 190 (2020) 12–27.
[42] K. Bharti, S. Manwal, C. Kishore, R.K. Yadav, P. Tiwari, D.B. Singh, Sensitivity analysis of N alike partly covered PVT flat plate collectors integrated double slope solar distiller unit, Desal. Water Treat., 211 (2021) 45–59.
[43] S.K. Sharma, A. Mallick, D.B. Singh, G.N. Tiwari, Experimental study of solar energy–based water purifier of single-slope type by incorporating a number of similar evacuated tubular collectors, Environ. Sci. Pollut. Res., 29 (2022) 6837–6856.
[44] D. Purnachandrakumar, G. Mittal, R.K. Sharma, D.B. Singh, S. Tiwari, H. Sinhmar, Review on performance assessment of solar stills using computational fluid dynamics (CFD), Environ. Sci. Pollut. Res., 29 (2022) 38673–38714.
[45] D. Kumar, R.K. Sharma, D.B. Singh, Effect of variation of mass-flow-rate and number of collectors on performance of active solar still, Desal. Water Treat., 248 (2022) 1–17.
[46] A. Raturi, R. Dobriyal, R.K. Sharma, A. Dwivedi, S.P. Singh, D.B. Singh, An investigation of effect of mass flow rate variation on productivity, exergoeconomic and enviroeconomic parameters on N similar PVTCPCs included with double slope solar still, Desal. Water Treat., 244 (2021) 12–26.
[47] V.S. Gupta, D.B. Singh, R.K. Mishra, S.K. Sharma, G.N. Tiwari, Development of characteristic equations for PVT-CPC active solar distillation system, Desalination, 445 (2018) 266–279.
[48] Shyam, G.N. Tiwari, I.M. Al-Helal, Analytical expression of temperature dependent electrical efficiency of N-PVT water collectors connected in series, Sol. Energy, 114 (2015) 61–76.
[49] D.B. Singh, G.N. Tiwari, Enhancement in energy metrics of double slope solar still by incorporating N identical PVT collectors, Sol. Energy, 143 (2017) 142–161.
[50] D.B. Singh, V.K. Dwivedi, G.N. Tiwari, N. Kumar, Analytical characteristic equation of N identical evacuated tubular collectors integrated single slope solar still, Desal. Water Treat., 88 (2017) 41–51.

[51] P.I. Cooper, Digital simulation of experimental solar still data, Sol. Energy, 14 (1973) 451–456.
[52] R.V. Dunkle, Solar Water Distillation, The Roof Type Solar Still and Multi-Effect Diffusion Still, International Developments in Heat Transfer, A.S.M.E., Proceedings of International Heat Transfer, Part V, University of Colorado, 1961, p. 895.
[53] P.K. Nag, Basic and Applied Thermodynamics, Tata McGraw-Hill, 2004, ISBN: 0-07-047338-2.
[54] D.B. Singh, Exergoeconomic and enviroeconomic analyses of N identical photovoltaic thermal integrated double slope solar still, Int. J. Exergy, 23 (2017) 347–366.
[55] D.B. Singh, N. Kumar, S. Kumar, V.K. Dwivedi, J.K. Yadav, G.N. Tiwari, Enhancement in exergoeconomic and enviro-economic parameters for single slope solar still by incorporating N identical partially covered photovoltaic collectors, J. Sol. Energy Eng. Trans. ASME, 140 (2018) 051002 (1–18), doi: 10.1115/1.4039632.
[56] Shyam, G.N. Tiwari, O. Fischer, R.K. Mishra, I.M. Al-Helal, Performance evaluation of N-photovoltaic thermal (PVT) water collectors partially covered by photovoltaic module connected in series: an experimental study, Sol. Energy, 134 (2016) 302–313.
[57] V.K. Dwivedi, G.N. Tiwari, Comparison of internal heat transfer coefficients in passive solar stills by different thermal models: an experimental validation, Desalination, 246 (2009) 304–318.
[58] D.B. Singh, G.N. Tiwari, Performance analysis of basin type solar stills integrated with N identical photovoltaic thermal (PVT) compound parabolic concentrator (CPC) collectors: a comparative study, Sol. Energy, 142 (2017) 144–158.
[59] D.B. Singh, N. Kumar, Harender, S. Kumar, S.K. Sharma, A. Mallick, Effect of depth of water on various efficiencies and productivity of N identical partially covered PVT collectors incorporated single slope solar distiller unit, Desal. Water Treat., 138 (2019) 99–112.
[60] G.N. Tiwari, Solar Energy, Fundamentals, Design, Modeling and Application, Narosa Publishing House, New Delhi, 2013.
[61] R. Petela, Exergy of undiluted thermal radiation, Sol. Energy, 74 (2003) 469–488.
[62] International Labor Office, Introduction to Work Study, International Labor Organization, Geneva, ISBN 81-204-0602-8, 1979.
[63] D.B. Singh, G.N. Tiwari, I.M. Al-Helal, V.K. Dwivedi, J.K. Yadav, Effect of energy matrices on life cycle cost analysis of passive solar stills, Sol. Energy, 134 (2016) 9–22.
[64] D.B. Singh, J.K. Yadav, V.K. Dwivedi, S. Kumar, G.N. Tiwari, I.M. Al-Helal, Experimental studies of active solar still integrated with two hybrid PVT collectors, Sol. Energy, 130 (2016) 207–223.

Appendix-A

Different unknown terms used in Eqs. (1)–(4) are as follows:

$$U_{\text{tca}}=\left[\frac{1}{h_o}+\frac{L_g}{K_g}\right]^{-1};U_{\text{tcp}}=\left[\frac{1}{h_i}+\frac{L_g}{K_g}\right]^{-1};$$

$$h_o=5.7+3.8V,\quad Wm^{-2}K^{-1};\quad h_i=5.7,\quad Wm^{-2}K^{-1};$$

$$U_{\text{tpa}}=\left[\frac{1}{U_{\text{tca}}}+\frac{1}{U_{\text{tcp}}}\right]^{-1}+\left[\frac{1}{h_i'}+\frac{1}{h_{pf}}+\frac{L_i}{K_i}\right]^{-1};$$

$$h_i'=2.8+3V,\quad Wm^{-2}K^{-1};$$

$$U_{L1}=\frac{U_{\text{tcp}}U_{\text{tca}}}{U_{\text{tcp}}+U_{\text{tca}}};\quad U_{L2}=U_{L1}+U_{\text{tpa}};$$

$$U_{\text{Lm}}=\frac{h_{\text{pf}}U_{L2}}{F'h_{\text{pf}}+U_{L2}};\quad U_{\text{Lc}}=\frac{h_{\text{pf}}U_{\text{tpa}}}{F'h_{\text{pf}}+U_{\text{tpa}}};$$

$$\text{PF}_1=\frac{U_{\text{tcp}}}{U_{\text{tcp}}+U_{\text{tca}}};\quad \text{PF}_2=\frac{h_{\text{pf}}}{F'h_{\text{pf}}+U_{L2}};$$

$$\text{PF}_c=\frac{h_{\text{pf}}}{F'h_{\text{pf}}+U_{\text{tpa}}};\quad (\alpha\tau)_{1\text{eff}}=(\alpha_c-\eta_c)\tau_g\beta_c;$$

$$(\alpha\tau)_{2\text{eff}}=\alpha_p\tau_g^2(1-\beta_c);\quad (\alpha\tau)_{\text{meff}}=\left[(\alpha\tau)_{2\text{eff}}+\text{PF}_1(\alpha\tau)_{1\text{eff}}\right];$$

$$(\alpha\tau)_{\text{ceff}}=PF_c.\alpha_p\tau_g;\quad A_m=WL_m;A_c=WL_c;$$

$$A_cF_{\text{Rc}}=\frac{\dot{m}_fc_f}{U_{\text{Lc}}}\left[1-\exp\left(\frac{-F'U_{\text{Lc}}A_c}{\dot{m}_fc_f}\right)\right];$$

$$A_mF_{\text{Rm}}=\frac{\dot{m}_fc_f}{U_{\text{Lm}}}\left[1-\exp\left(\frac{-F'U_{\text{Lm}}A_m}{\dot{m}_fc_f}\right)\right];$$

$$\left(AF_R(\alpha\tau)\right)_1=\left[A_cF_{\text{Rc}}(\alpha\tau)_{\text{ceff}}+\text{PF}_2(\alpha\tau)_{\text{meff}}A_mF_{\text{Rm}}\left(1-\frac{A_cF_{\text{Rc}}U_{\text{Lc}}}{\dot{m}_fc_f}\right)\right];$$

$$\left(AF_RU_L\right)_1=\left[A_cF_{\text{Rc}}U_{\text{Lc}}+A_mF_{\text{Rm}}U_{\text{Lm}}\left(1-\frac{A_cF_{\text{Rc}}U_{\text{Lc}}}{\dot{m}_fc_f}\right)\right];$$

$$K_K=\left(1-\frac{\left(AF_RU_L\right)_1}{\dot{m}_fc_f}\right);\quad \left(AF_R(\alpha\tau)\right)_{m1}=\text{PF}_2(\alpha\tau)_{\text{meff}}A_mF_{\text{Rm}};$$

$$\left(AF_RU_L\right)_{m1}=A_mF_{\text{Rm}}U_{\text{Lm}};\quad K_m=\left(1-\frac{A_mF_{\text{Rm}}U_{\text{Lm}}}{\dot{m}_fc_f}\right);$$

$$(\alpha\tau)_{\text{eff},N}=\frac{\left(AF_R(\alpha\tau)\right)_1}{(A_c+A_m)}\left[\frac{1-(K_K)^N}{N(1-K_K)}\right];$$

$$U_{\text{L,N}}=\frac{\left(AF_RU_L\right)_1}{(A_c+A_m)}\left[\frac{1-(K_K)^N}{N(1-K_K)}\right]$$

Different unknown terms used in Eqs. (5)–(14) are as follows:

$$a_2=\frac{1}{M_wC_w}\left[\dot{m}_fC_f\left(1-K_k^N\right)+U_bA_b+\frac{h_{1\text{wE}}(P-A_2)A_b}{2P}+\frac{h_{1\text{wW}}(P-B_2)A_b}{2P}\right];$$

$$\bar{f}_2(t)=\frac{1}{M_w C_w}\left[\left(\frac{\alpha'_w}{2}+h_1\alpha'_b\right)A_b\left(\bar{I}_{\mathrm{SE}}(t)+\bar{I}_{\mathrm{SW}}(t)\right)+\frac{\left(1-K_k^N\right)}{\left(1-K_k\right)}\left(\mathrm{AF}_R(\alpha\tau)\right)_1\bar{I}_c(t)+\left(\frac{\left(1-K_k^N\right)}{\left(1-K_k\right)}\left(\mathrm{AF}_R U_L\right)_1+U_b A_b\right)\bar{T}_a+\left(\frac{h_{1\mathrm{wE}}A_1+h_{1\mathrm{wW}}B_1}{P}\right)\frac{A_b}{2}\right];$$

$$A_1=R_1U_1A_{\mathrm{gE}}+R_2h_{\mathrm{EW}}A_{\mathrm{gW}};\qquad A_2=h_{1\mathrm{WE}}U_2\frac{A_b}{2}+h_{\mathrm{EW}}h_{1\mathrm{WW}}\frac{A_b}{2};$$

$$P=\left(U_1U_2-\frac{h_{\mathrm{EW}}^2}{A_{\mathrm{gE}}}h_{1\mathrm{WW}}\frac{A_b}{2}\right)A_{\mathrm{gW}};\qquad U_1=\frac{h_{1\mathrm{wE}}\frac{A_b}{2}+h_{\mathrm{EW}}A_{\mathrm{gE}}+U_{c,\mathrm{gaE}}A_{\mathrm{gE}}}{A_{\mathrm{gW}}};$$

$$U_2=\frac{h_{1\mathrm{wW}}\frac{A_b}{2}+h_{\mathrm{EW}}A_{\mathrm{gW}}+U_{c,\mathrm{gaW}}A_{\mathrm{gW}}}{A_{\mathrm{gE}}};\qquad B_1=\frac{\left(R_2P+A_1h_{\mathrm{EW}}\right)A_{\mathrm{gW}}}{U_2A_{\mathrm{gE}}}$$

$$B_2=\frac{\mathrm{Ph}_{1\mathrm{wW}}\frac{A_b}{2}+h_{\mathrm{EW}}A_{\mathrm{gW}}A_2}{U_2A_{\mathrm{gE}}};\qquad R_1=\alpha'_gI_{\mathrm{SE}}(t)+U_{c,\mathrm{gaE}}T_a;$$

$$R_2=\alpha'_gI_{\mathrm{SW}}(t)+U_{c,\mathrm{gaW}}T_a$$

$$h_{\mathrm{EW}}=0.034\times5.67\times10^{-8}\left[\left(T_{\mathrm{giE}}+273\right)^2+\left(T_{\mathrm{giW}}+273\right)^2\right]\left[T_{\mathrm{giE}}+T_{\mathrm{giW}}+546\right]$$

$$U_{c,\mathrm{gaE}}=\frac{\frac{K_g}{l_g}h_{1\mathrm{gE}}}{\frac{K_g}{l_g}+h_{1\mathrm{gE}}};U_{c,\mathrm{gaW}}=\frac{\frac{K_g}{l_g}h_{1\mathrm{gW}}}{\frac{K_g}{l_g}+h_{1\mathrm{gW}}};$$

$$h_{1\mathrm{gE}}=5.7+3.8V;\quad h_{1\mathrm{gW}}=5.7+3.8V;$$

$$h_{1\mathrm{wE}}=h_{\mathrm{rwgE}}+h_{\mathrm{cwgE}}+h_{\mathrm{ewgE}};$$

$$h_{1\mathrm{wW}}=h_{\mathrm{rwgW}}+h_{\mathrm{cwgW}}+h_{\mathrm{ewgW}};$$

$$h_{\mathrm{ewgE}}=16.273\times10^{-3}h_{c,\mathrm{wgE}}\left[\frac{P_w-P_{\mathrm{giE}}}{T_w-T_{\mathrm{giE}}}\right];$$

$$h_{\mathrm{cwgE}}=0.884\left[\left(T_w-T_{\mathrm{giE}}\right)+\frac{\left(P_w-P_{\mathrm{giE}}\right)\left(T_w+273\right)}{268.9\times10^3-P_w}\right]^{\frac{1}{3}};$$

$$h_{\mathrm{ewgW}}=16.273\times10^{-3}h_{c,\mathrm{wgW}}\left[\frac{P_w-P_{\mathrm{giW}}}{T_w-T_{\mathrm{giW}}}\right];$$

$$h_{\mathrm{cwgW}}=0.884\left[\left(T_w-T_{\mathrm{giW}}\right)+\frac{\left(P_w-P_{\mathrm{giW}}\right)\left(T_w+273\right)}{268.9\times10^3-P_w}\right]^{\frac{1}{3}};$$

$$P_w=\exp\left[25.317-\frac{5144}{T_w+273}\right];$$

$$P_{\mathrm{giE}}=\exp\left[25.317-\frac{5144}{T_{gi}E+273}\right];$$

$$P_{\mathrm{giW}}=\exp\left[25.317-\frac{5144}{T_{\mathrm{giW}}+273}\right];$$

$$h_{\mathrm{rwgE}}=\left(0.82\times5.67\times10^{-8}\right)\left[\left(T_w+273\right)^2+\left(T_{\mathrm{giE}}+273\right)^2\right]\left[T_w+T_{\mathrm{giE}}+546\right];$$

$$h_{\mathrm{rwgW}}=\left(0.82\times5.67\times10^{-8}\right)\left[\left(T_w+273\right)^2+\left(T_{\mathrm{giW}}+273\right)^2\right]\left[T_w+T_{\mathrm{giW}}+546\right];$$